Application of Computational Fluid Dynamics Technique in Food Value Addition: A Case of Cake Baking using Cassava Flour

By

Nekesa Diana

BU/GS21/MIM/6

A Dissertation Submitted to the Directorate of Graduate Studies, Research and Innovation in Partial Fulfilment for the Requirements of the Award of the Degree of Master of Science in Industrial Mathematics of Busitema University

October 2024

Declaration

I, NEKESA DIANA hereby certify that this dissertation is a result of my original research work and to the best of my knowledge it has never been submitted for any degree award in any other university before and I present it without any reservations for external examination.

Name: NEKESA DIANA

Signature: .....

Date: 28th/10/2024

Approval

This dissertation has been submitted for examination with the approval of the following supervisors.

1. Dr. Rebecca Muhumuza Nalule

   Department of Mathematics

   Busitema University

   Signature: .....

   Date: 28-10-2024

2. Dr. Annet Kyomuhangi

   Department of Mathematics

   Busitema University

   Signature: .....

   Date: 29/10/2024

Dedication

This research work is dedicated to my father, Late Oguttu Were Jackson, may God continue to grant you eternal rest.

Acknowledgements

First and foremost, all praise and adoration belong to the almighty God for the gift of life, good health, wisdom, provision and protection rendered to me throughout my study. For it is only by His grace that I have been able to come this far.

I wish to express my gratitude to Busitema University, more specifically, the Faculty of Science and Education, Nagongera Campus for giving me the opportunity to undertake this course.

My sincere and deepest gratitude goes to my supervisors; Dr. Rebecca Muhumuza Nalule and Dr. Annet Kyomuhangi. Their sage advice, continuous stream of ideas, insightful criticisms and encouragement helped in the writing of this dissertation. They have been inspirational in allowing me to freely investigate while keeping me focused at the same time. Their interest helped my enthusiasm towards completing this research.

Special thanks to the staff in the Department of Mathematics, Busitema University for the great impact in education. To the head, Department of Mathematics, Dr. Abubakar Mwasa, thank you for always attending our seminar series physically and encouraging us; Dr. Asaph Keikara Muhumuza the Coordinator of Master of Science in Industrial Mathematics (MIM) programme for continuously listening to our challenges and guiding us, Dr. Fulgensia Mbabazi, Dr. Stephen Kadedesya and Dr. Joseph Ddumba Lwanyaga for your valuable support.

I also thank Dr. Anselm Oyem for his invaluable guidance and continuous support which have been of great value to my growth and success in this research.

My sincere gratitude goes to my wonderful MIM classmates at Busitema University; (Sarah Kobusinge, Samuel Kirabe, Emmanuel Wafula and Godfrey Izizinga) for their valuable help. May God bless you abundantly.

Finally, words can not do enough justice for my immense and eternal gratitude to my mother, Mrs. Nandera F. Oguttu, my sisters, Brenda Anyango and Vanessa Nabooli, my brothers, Patrick Barasa, John Ojambo and Edward Bwire; my friends Lydiah Amoit, Tulirinya John and Roggers Waibi for their endless and unconditional love and support. Thank you very much! May God reward you all abundantly.

Contents

List of Figures

List of Tables

Acronyms And Abbreviations

ANOVA	:	Analysis of Variance
CAVA	:	Cassava Adding Value for Africa
CFD	:	Computational Fluid Dynamics
CG	:	Cynogenic Glycocides
EA	:	East Africa
FAO	:	Food and Agricultural Organisation
FEM	:	Finite Element Method
FVM	:	Finite Volume Method
FRI	:	Food Research Institute
GI	:	Glycemic Index
HQCF	:	High Quality Cassava Flour
HRCS	:	Highly enzyme Resistant Cassava Starch
NS	:	Navier Stokes
NRI	:	Natural Research Institute
PDEs	:	Partial Differential Equations
PPD	:	Post harvest Physiological Disorder
SDGs	:	Social Development Goals
COMSOL	:	Computational Solutions

Nomenclature

Symbol	Description	Units
K_α	Reaction Rate Constant	per second (s^{-1})
K_0	Pre-Exponential Factor	per second (s^{-1})
R	Gas Constant	Joule per Mole per Kelvin (J mol^{-1} K^{-1})
E	Activation Energy	Joule per Mole (J mol^{-1})
T	Temperature	Kelvin
m	Mass of the fluid element	Kilograms (kg)
ρ	Density of the fluid	kg m^{-3}
ρ_g	Density of the gas	kg m^{-3}
v	Fluid Velocity	m s^{-1}
P	Pressure	Pascal (Pa)
f	Body Force	Newton (N)
λ	Effective Thermal Conductivity	W m^{-1} K^{-1}
$\triangle K$	Phase Change Rate	kg s^{-1}
C_p	Specific Heat Capacity at constant pressure	J kg^{-1} K^{-1}
$C_{p,g}$	Specific Heat Capacity of the gas at constant pressure	J kg^{-1} K^{-1}
L_v	Latent heat of vaporization	J kg^{-1}
u	Inlet Velocity Component in the x direction	m s^{-1}
v	Inlet Velocity Component in the y direction	m s^{-1}
w	Inlet Velocity Component in the z direction	m s^{-1}
σ	Normal Stress	N m^{-2}
τ	Shear Stress	N m^{-2}
a	Acceleration	m s^{-2}
μ	Dynamic Viscosity	Pa s
g	Acceleration due to gravity	m s^{-2}
C	Specific Heat	J kg^{-1} K^{-1}
δ	Stefan-Boltzmann Universal Constant	W m^{-2} K^4
ε	Emissivity	-
α	Degree of Gelatinization	-
∇^2	Scalar differential operator (Laplacian)	-

Abstract

Cassava flour cake baking entails changes in temperature, moisture content and volume, which are closely linked aspects in the heat and mass transfer phenomena that take place during the baking process. This process of baking is often faced with challenges related to texture and structure. Computational Fluid Dynamics is therefore utilized in this study to determine the temperature and moisture content profiles during cake baking using cassava flour in dough formation. A mathematical model was applied in the baking process and solved using CFD technique employing the Finite Element Method (FEM) so as to optimize baking conditions, that is baking temperature, time and moisture content. Using COMSOL Multiphysics software (version 6.2), simulation results showed that as the oven temperature and temperature within the dough increase, moisture content reduces. Additionally, results also reveal that the temperature distribution within the dough increases with baking time. This study established an optimal baking time of 45 minutes at a temperature of 453K leaving a moisture content of $0.24KgKg^{-1}$. Moreover, simulated results were in agreement with those in different studies on baking using wheat flour. Based on the findings, we recommend the adoption of CFD simulations in standardizing cassava cake baking and integrating value added ingredients for improved nutritional value to give cassava a much bigger market value.

Key words: Cassava Cake Baking, CFD, Multiphase Flow, FEM

Chapter 1

INTRODUCTION

In recent years, food processing has become essential since the world is facing challenges concerning food security, quality and sustainability. As the demand for processed food rises, understanding food processing principles is required. Therefore, this chapter explores the relationship between food processing and mathematical modeling, specifically through the use of CFD.

1.1 Background of Study

Food processing is the act of performing a sequence of mechanical or chemical processes on agricultural products in order to change them from one form or state to another or to preserve them (Therdthai, Zhou, & Adamczak, 2004). Some of the food processing methods include; pasteurisation, drying, smoking, canning, freezing, milling (Anandharamakrishnan & Anandharamakrishnan, 2013). In all food processing practices like freezing, drying, sterilisation, spraying and baking, the fluid flow can be explained by taking into account the conservation laws of mass, momentum and energy balances, which result into a set of partial differential equations Versteeg and Malalasekera (1995), indicating that the flow under consideration can be modeled and simulated. Since fluid problems become more complex, the unsteady state momentum, heat and mass transfer PDEs can be solved numerically under some assumptions because, the participation of concurrent mechanical, chemical and biological dynamics in the processing of food, makes modeling such processes very complex given that there is limited knowledge and doubts about the different food properties. Hence, the aim of any mathematical representation is to absorb significant characteristics of a complicated procedure depending on the current conceptual knowledge about the case under study since it is not possible to put every single parameter into consideration (Chhanwal, Tank, Raghavarao, & Anandharamakrishnan, 2012; Trystram, 2012).

Mathematical modeling is the process of transforming a real life problem into a mathematical language and then solving the problem to obtain a real life solution (Kapur, 2023). Since mathematical modeling looks forward to gaining an understanding of science by using mathematical equations and simulations, it has emerged as a powerful essential tool for studying a variety of problems in scientific,

engineering and industrial researches, products and process improvement (Chhanwal et al., 2012). These essential tools include; identifying the problem, translating the problem into a model, derive from the model to mathematical equations (mathematical model), transform the mathematical model into a computational model, simulate, and obtain results, then check the validity of the results whether the solutions obtained meets the real world problem (Velten, Schmidt, & Kahlen, 2024).

Most food products have their thermophysical properties like density, viscosity, among others, varied during processing which then depend on velocity, temperature, space and time (Chhanwal et al., 2012). Time and temperature have a significant impact on processing outcomes, suggesting that a thorough understanding of the interactions that take place during processing and the changes brought about by the parameters established is essential to achieving the intended product quality and nutritional content (Therdthai et al., 2004; Yanniotis & Stoforos, 2014; Chakraborty & Dash, 2023).

Computational Fluid Dynamics has emerged as the most powerful instrument for obtaining numerical solutions to equations governing the fluid flow (Scott & Richardson, 1997; Norton & Sun, 2006; Park & Yoon, 2018). It can be used in various processing industries like, chilling and refrigeration, spray drying, freeze drying, baking, pasteurization/sterilization, heat exchangers and mixing (Scott & Richardson, 1997) and its use is rapidly growing. Additionally, it can be used in the design and optimization of devices such as coolers, heat exchangers, ovens and spray dryers, processes including heating, cooling, freezing, drying and baking are cumulative (Anandharamakrishnan & Anandharamakrishnan, 2013).

The implementation of CFD has been unavoidable and advancing over time. The desire to get effective, in-depth findings has always been prohibited by the high expenses and time commitment that comes along with testing (Xia & Sun, 2002). Furthermore, related assumptions and estimations have also inhibited analytical models from creating all-inclusive flow solutions (Versteeg & Malalasekera, 1995). Relating such restrictions with the latest advancements in processing power and efficiency, as well as the development of numerical solutions for the Navier-Stokes equations, provides a basis for understanding the reasons why using CFD has become a feasible substitute, particularly in the food sector (Batchelor, 2000).

The application of Computational Fluid Dynamics has been used in different cases, such as; baking (Therdthai et al., 2004; Mirade, Daudin, Ducept, Trystram, & Clément, 2004; Anishaparvin, Chhanwal, Indrani, Raghavarao, & Anandharamakrishnan, 2010; Chhanwal et al., 2012), design and improvement of dryers, ovens and chillers (Norton & Sun, 2006). These authors highlighted the importance of CFD in

their documentations and they concluded that it is an extremely powerful tool for enhancing the overall procedure and final product quality within the food processing sector. There is a strong correlation between CFD and the food and beverage sector procedure such as chilling, sterilisation, drying, cold storage and mixing (Khan et al., 2022). These processes are frequently employed to improve food items' quality, safety and shelf life (Shittu, Alimi, Wahab, Sanni, & Abass, 2016; Szpicer, Bińkowska, Wojtasik-Kalinowska, Salih, & Półtorak, 2023).

Cassava, scientifically known as *Manihot esculenta* is a tuberous root of a humid tree used for food in many countries of the world (Rogers, 1963). It is spread by cutting the stems into segments and planting them before the rainy season. Cassava plant, grows to approximately 1-4 metres in height and cultivated for its roots and leaves which are sometimes processed and eaten as food. Following rice and maize, as the third source of foods rich in carbohydrates, cassava is one of the basic foods in many countries (Fauquet & Fargette, 1990; Sengar, 2022). The cassava crop is drought resistant and can grow even on soils with low fertility (Oladunmoye, Aworh, Maziya-Dixon, Erukainure, & Elemo, 2014; Kuye & Ettah, 2016).

Figure 1.1: Cassava plantation

Nigeria is Africa's top producer of cassava, with Democratic Republic of Congo in the second place and then Ghana while in East Africa (EA), the biggest producer of cassava is Tanzania , which is followed by Uganda as per Food and Agricultural Organisation statistics (Adebayo, 2023).

Figure 1.2: Fresh tubers of cassava roots (https://www.greenharvest.com.au)

Figure 1.3: (a) Peeled, sliced and dried cassava - (b) Processed powered cassava (https://cassavaradise.en.ec21.com)

In Uganda, cassava is a main food crop that is consumed extensively throughout the nation, especially in the Northern and Eastern regions (Haggblade & Dewina, 2010). The traditional growing areas of cassava include West Nile, North and Eastern parts of the country which is now increasingly being grown in the Western and Southern regions. Cassava is eaten by both humans and animals, and also extensively utilized in the food sector, textile industry, paper making, glue, alcohol, sweeteners and starch (Abass et al., 2017). It also has the likelihood of being processed into high quality foods like snacks to meet the growing demand from consumers. It is also a source of household income.

Cassava is in two varieties, namely; sweet type and bitter kind (Adebayo, 2023). Both varieties are alike in terms of cultivation and overall appearance except that the sweet type contains a smaller

quantity of cyanide compounds (less poisonous) which does not require much processing while the bitter type produces much higher amounts of cyanide compounds (more toxic) (Cooke, 1978). It is detached by simple drying to diminish the acidic level, soaking the cassava in water first such that the cyanide is filtered out and by boiling before cassava is consumed (Maduagwu & Adewale, 1981; Mahungu, Yamaguchi, Almazan, & Hahn, 1987). Traditionally, cassava is stored in various ways such as; re-burying the cassava under the ground, storing it in granaries and soaking it in water. Customarily, cassava is processed before consumption thereby reducing the cyanogenic glucosides which exist in fresh cassava especially for the bitter variety. Processing yields products that have different features which creates variety in cassava foods such as cassava flour, fried cassava chips, starch hence widening the consumers' choice (Odebode, 2008).

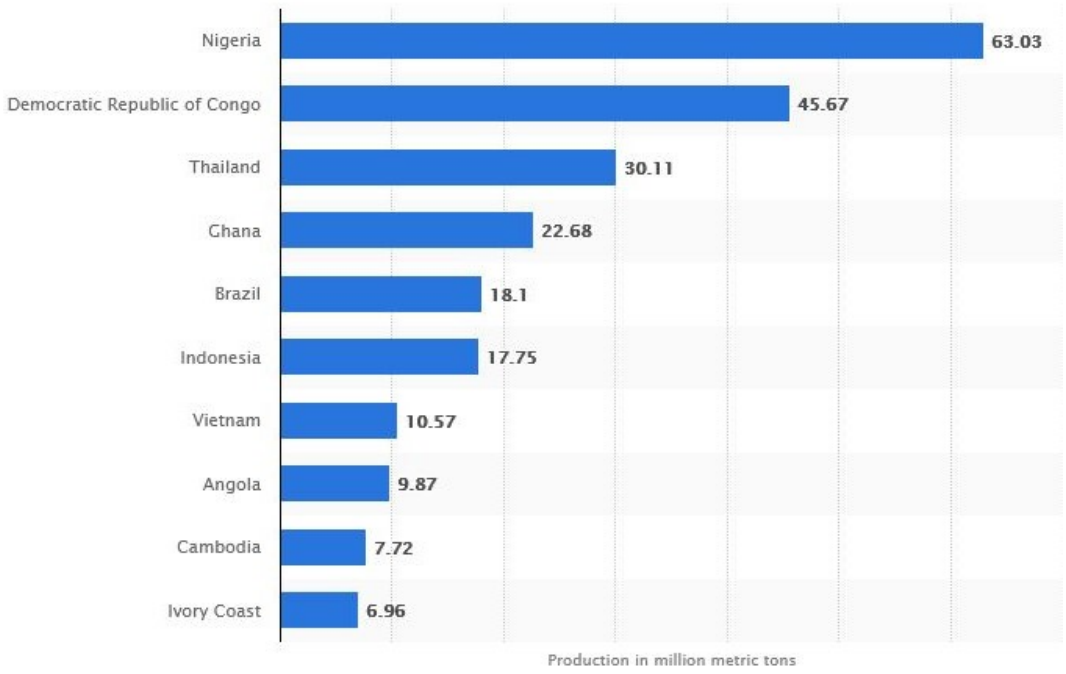

Figure 1.4: Global cassava production statistics (FAO, 2021)

Cassava, being a staple food is linked to people's day to day living. The consumable fleshy part of cassava root consists of 25% carbohydrates, 62% water, 0.3% fat, (1-2)% protein, (1-2)% fibre and 1% mineral matter, and the biggest percentage of carbohydrates comprises of starch (Onwueme, 1978; Bayata, 2019).

Baking cassava cakes is a food processing method whereby a series of intricate mechanical and biochemical alterations concurrently occur in manufacturing the end product (Therdthai et al., 2004). The quality of any bakery final product depends on its moisture content, texture, colour, shape and size

but all the above elements are temperature dependent (Yanniotis & Stoforos, 2014). While in the baking process, an oven is very essential since it assists as a basis of energy leading to heat and mass transfer process (Rahman, Nassef, Rezk, Assad, & Hoque, 2021). This suggests any bakery product's quality can be determined by optimizing the oven temperature (Zhou & Therdthai, 2018). Understanding the mass and heat transfer mechanism through mathematical modeling is crucial in designing ovens, enhancing energy efficiency, optimizing processes and ensuring product quality (Süfer, Kumcuoğlu, & Tavman, 2016). (Navacchi, de Carvalho, Takeuchi, & Danesi, 2012) in the process of making a cassava cake, used processed cassava flour, eggs, sugar, margarine, spirulina platensis and cassava bran were used and diverse preparations of cassava cake were established while altering the concentration of the cassava bran and spirulina platensis. These materials were mixed together to obtain homogeneous dough thereby determining the volume of the dough, v_1 from;

$$v_1 = a \times b \times c \tag{1.1}$$

where length is represented by a, width by b is width and height by c.

Dough was then separated into portions of 1 Kg and placed in aluminium rectangular baking trays of stipulated sizes, and baked in an electric oven. After baking, the volume of the baked cake v_2 was obtained by

$$ER = \left(\frac{v_2 - v_1}{v_1} \right) \times 100\% \tag{1.2}$$

$$v_2 = v_1 \left[ER + 1 \right] \times 100\% \tag{1.3}$$

where ER is expansion rate.

Value addition refers to the transformation of raw products into higher value goods or changing something from its original form to a high quality state which enhances the overall end product (Ani, Ojila, & Abu, 2019), say, processing maize into flour and packing it, drying herbs and grinding them into powder, manufacturing of perfumes from flowers, trees in the making of furniture, paper, among others. Value addition in this study is vital because it provides improved nutrition, extended storage which minimises wastage and ensures greater food security. It also creates employment opportunities for people in food processing industries like the food processors, industrial chemists.

1.2 Statement of the Problem

Cassava, one of the staple foods in Uganda, is commonly consumed as boiled fresh cassava, a mixture of cassava and beans (”katogo”) or fried cassava chips. Dry cassava can also be processed into flour which is used for home consumption in making ‘kalo’ after being mingled as plain flour or for commercial sale. With increased cassava yield varieties, there is high production of cassava locally and regionally. However, bakers face challenges when using cassava flour to make cakes since the results often do not meet the desired quality. This is partly because the cake’s quality is impacted by the underlying heat and mass transfer mechanism which occurs during baking.

1.3 Objectives of the study

1.3.1 Main objective

To create a mathematical framework which incorporates cassava flour as the primary component in dough formation in the cake baking process, focussing on analysing the changes in temperature and moisture content profiles using CFD so as to determine the ideal baking conditions.

1.3.2 Specific Objectives

The specific objectives of the study are;

1. To incorporate cassava flour into a mathematical model for cake baking.
2. To determine the moisture content and temperature profiles during baking.
3. To establish the optimal conditions necessary in a baked cake from cassava flour.

1.4 Research questions

i) Which mathematical model is applicable for cake baking?

ii) Which technique of CFD can be used to solve the model?

iii) Under what conditions can we obtain the best product after the baking process?

1.5 Significance of the Study

From the food value addition aspect to cassava in terms of cake baking using cassava flour, the research output will be beneficial to the country at large with cassava farming communities being the primary beneficiaries since they are directly involved in its production including cassava processors. It is through adding value to agricultural products such as cassava that the food processing industry is capable of providing a range of higher quality goods like bread, cakes, glue, sweeteners, animal feeds, alcohol and starch with improved nutrition which provides a wide range of choice to consumers. It also improves the taste, helps in the removal of toxins and increases the shelf life of cassava. This implies that the dependence on cassava will to a higher degree rely on how better it can be transformed into different forms at competitive prices that are relative to other substitute goods. There will be employment opportunities to individuals in the food processing industry like the food bakery workers, chemical engineers, canning and preserving industry workers, confectionery industry workers, cooks and chefs, food technologists and packaging engineers. It is also a source of revenue to the government through taxation. This case of study may also play a role in attaining the SDGs of 2030 such as no hunger, no poverty, good health and well being in the communities. It is also a source of practical knowledge which can be adapted by the food processing industry to increase production leading to economic growth and development.

1.5.1 Conceptual Structure

The study's conceptual structure was summarized as per the flow chart Figure 1.5 and characterized by Mathematical theories and the key concepts.

1.5.2 Definition of Terms

(i) **Applied Mathematical Analysis :** Mathematical models used in the baking process are employed in terms of space and time. The space variable is usually a distance measure. Therefore, we employ such principles of Applied Mathematical Analysis including metric distance, continuity considering the continuum hypothesis (the fluid is treated as a continuum) (Süfer et al., 2016) and convergence since factors like temperature, pressure, velocity, viscosity are controlled by Mathematical analysis especially the optimal points).

(ii) **Principle of Fluid Dynamics :** It provides a basis for categorizing the kind of fluid flow under

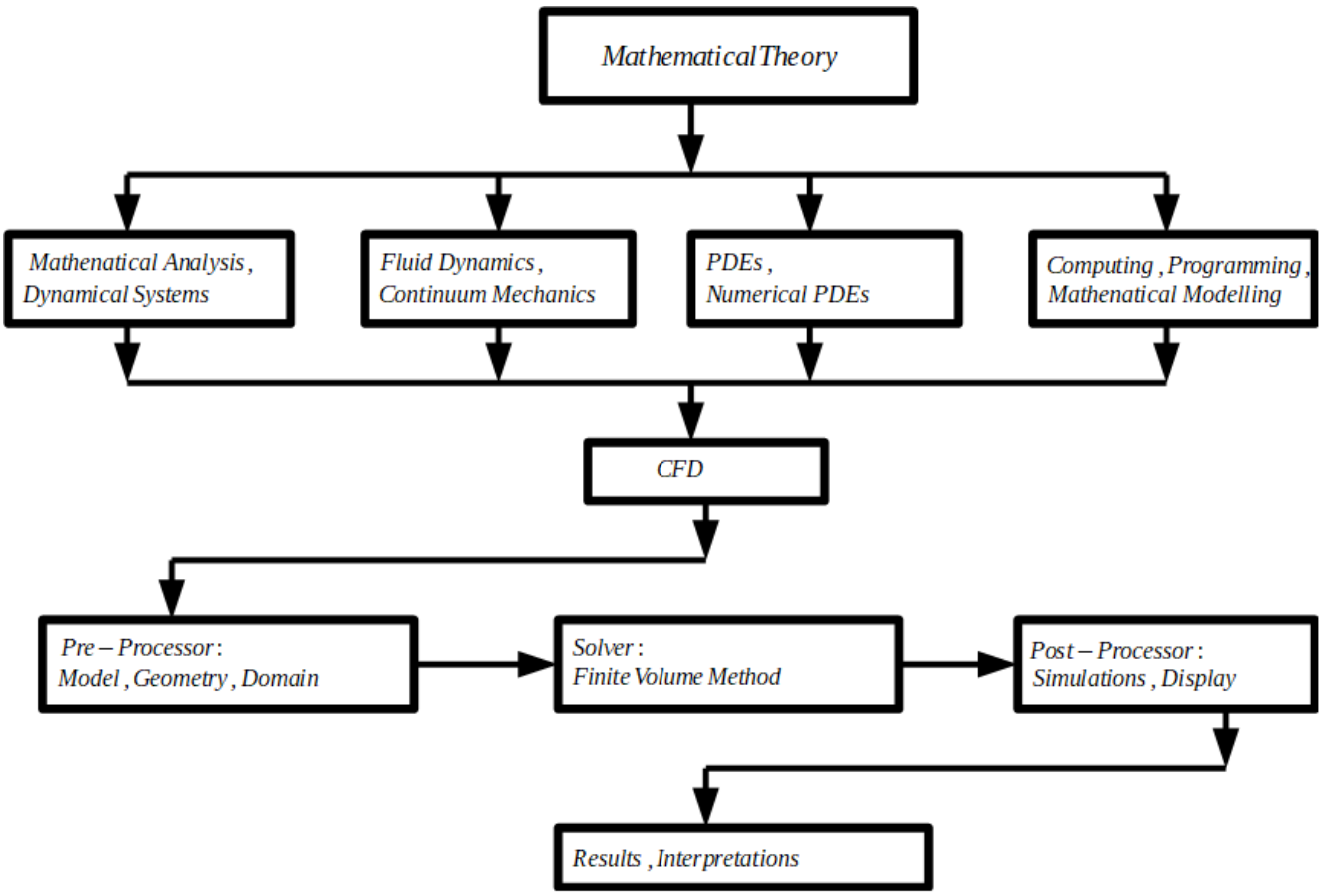

Figure 1.5: Conceptual framework

study. Different types of fluid flow may include: steady or unsteady, rotational or irrotational, laminar or turbulent flow (Al-Nasser, Fayssal, & Moukalled, 2021). In the baking process, this study deals with an unsteady, rotational and turbulent fluid flow (Batchelor, 2000) .

(iii) **Continuum Mechanics :** From the microscopic perspective, a fluid is composed of individual molecules. The molecules have the same mass but each molecule has its own velocity, temperature and other fluid properties during motion (Chhanwal et al., 2012). This implies that the different molecules have different equations hence generating a large number of equations whose simplification may be complex. From the macroscopic approach, we fix our attention to the quantity of matter (substance) without going into events occurring at molecular level. We are concerned with the gross or average behaviour of all the molecules. This approach greatly reduces the complexity of the problem. This explains the assumption of treating the fluid as a continuum (Batchelor, 2000).

(iv) **Partial Differential Equations (PDEs) :** An equation involving two or more variables and some of its partial derivatives is called a PDE (Trystram, 2012). We can employ a family of PDE's

which are non linear (a case of the Navier-Stokes equations) which control fluid flow accounting for velocity, density, momentum, pressure, viscosity and heat transfer (Sharma, 2021).

(v) **Numerical Solutions of PDE's :** These involve the numerical techniques employed in solving a set of PDE's describing the transfer of heat and mass during baking. The numerical techniques include: Finite Volume Method, Finite Element Method and Finite Difference Method (Al-Nasser et al., 2021).

(vi) **Principles of Computer Programming :** Due to the complexity of the nonlinear PDE's, a special type of the Navier-Stokes equations, this study will employ numerical techniques which require programming through which simulations are done (Chakraborty, Routray, & Dash, 2022) .

(vii) **Computational Fluid Dynamics:**CFD basically uses computer based simulations to solve problems that comprise fluid flow, heat transfer Sharma (2021) besides related occurrences like chemical reactions. In the baking process, the fluid (dough) is subjected to heat under certain conditions such that the final product (cake) is obtained. Since it is not easy to get an analytical solution for the set of PDE's that describe the processes of heat and mass transport during baking, numerical methods and computer simulations set in (Tu, Yeoh, Liu, & Tao, 2023).

In conclusion, food processing has become essential since the world is facing challenges concerning food security, quality and sustainability. As the demand for processed food rises, understanding food processing principles is required. Therefore, this chapter explores the relationship between food processing and mathematical modeling, specifically through the use of CFD. The next Chapter 2, the literature review of the major scientific research studies that involve utilizing CFD in food processing, specifically, cake baking.

Chapter 2

LITERATURE REVIEW

This chapter discusses the vital contributions that different researchers have made towards food processing while using traditional methods and advanced techniques. The application of CFD in food value industrial processes has gained significant attention. Thus it has offered an encouraging instrument for optimization of different processes of food production thereby enhancing the quality of the product. This chapter on literature review explored the present state of scientific knowledge and research on the use of CFD while adding value to food.

2.1 Cassava processing

World wide, bakery products including cakes, bread, biscuits, doughnuts, cookies, pies among others are usually made out of wheat flour which is in most cases imported. Dziedzoave (1998) highlighted the dominance of wheat compared to other categories of baking flour hence monopolising the global market.

Navacchi et al. (2012) portrayed that interest in composite flour was sparked by the growing demand for wheat baked goods in many developing countries despite their incapacity to produce enough wheat Their goal was to increase use of the locally available starchy flour.

The CAVA was implemented in five (5) African countries namely; Uganda, Ghana, Malawi, Nigeria and Tanzania. Its major aim was to increase the production of cassava in terms of volumes and value, discovered more avenues of increasing the use of cassava creating value chains for premium cassava flour in order to raise earnings and improve the standard of living for those engaged in the processing and production (Adebayo, 2023). For instance in Ghana, the Department for International Development sponsored a joint project performed by NRI and FRI so as to utilize the industrial potential of cassava. This was done by training farmers on the methods of processing fresh cassava into HQCF. Research portrays that in the process of manufacturing bakery products, wheat flour can either be fully or to a certain percentage be replaced by HQCF (Tien, Duyen, & Hung, 2019). Processing of cassava roots into HQCF requires steps as shown in Figure 2.1.

The University of Ghana together with the Natural Research Institute (NRI) and Food Research

Institute (FRI) through Dziedzoave (1998) carried out a research on the impact of the use of HQCF as replacement of wheat in the manufacture of soft and hard dough biscuits from two bakeries in Accra. It was found that in soft biscuits, High Quality Cassava Flour substituted 35% of wheat flour while for hard biscuits, HQCF replaced 60% of wheat flour. It was also noted that the substitution of HQCF had no impact on the final products' quality. This provided a wider market for high quality cassava flour in the food processing industry.

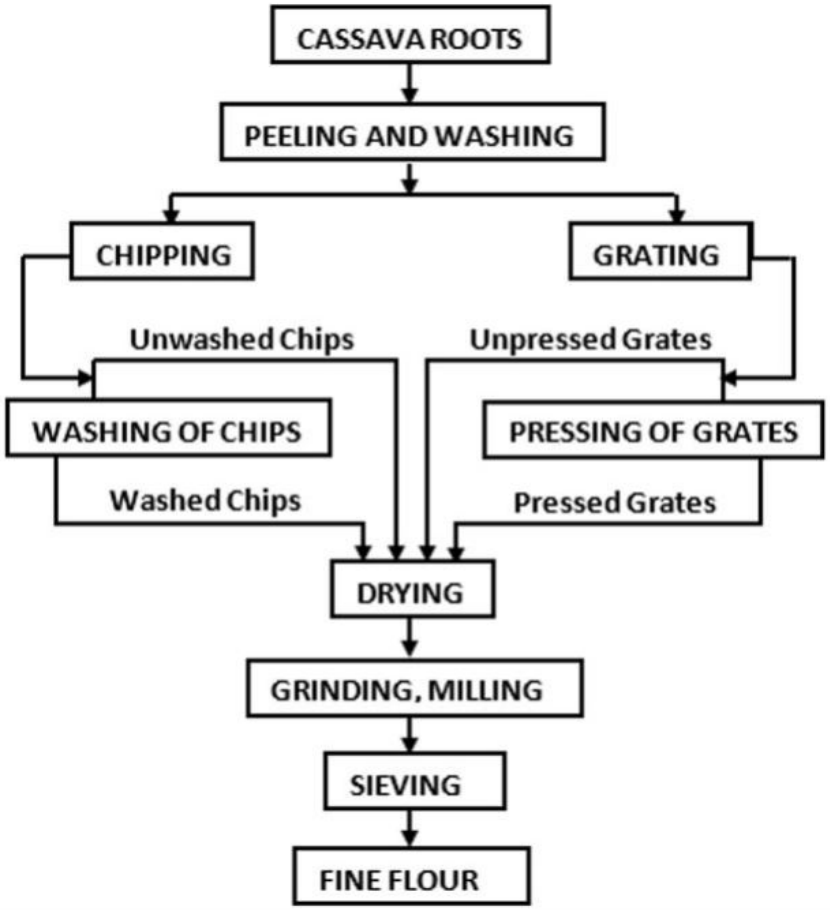

Figure 2.1: Flow diagram of cassava flour production using different primary processing techniques (Orias & Calub Jr, 1986).

Questionnaires were used in Navacchi et al. (2012) to make suitable comparison between the standard recipe and the prepared or formulated recipes. Baked cake samples were served to students in a public school as well as questionnaires given to get their responses towards the taste of the different cake recipes. The results presented an outstanding acceptance which made viable growth of the baked cake because of its nutrition. The study on post harvest storage, handling and processing of cassava root and its bi-products by Uchechukwu-Agua, Caleb, and Opara (2015) revealed that since cassava flour is free from gluten, it could be used in the manufacture of vital foods like bread and cakes. The study also considered

the importance of prime post harvest handling, processing and storage practices which if were put into practice, would relieve certain anxieties of food insecurity. Moreover, it was also revealed in Abass et al. (2017) that if cassava processing was mechanized rightly, it generated more demand that modified primary production for hiked yields, efficiency in production and hence higher incomes.

In Parmar, Sturm, and Hensel (2017), it was indicated that cassava developed gradually as a raw ingredient utilized in the production of starch in comparison to other cash crops. Unteawati and Fatih (2018) showed that the demand for cassava from rural areas was very high and this triggered more local production. The study also depicted that consumers preferred cassava chips to other cassava recipes (Ubalua & Mbanaso, 2013). These studies revealed that the growth of cassava was mainly affected by post-production processes highlighted as PPD and CG. The study by Parmar et al. (2017) also portrayed that there was an ongoing collaborative research on participatory plant breeding whose aim was to come up with resistant varieties, reduce the levels of PPD and CG, then improve nutritional values.

An investigation on the production of cassava, its processing and nutritional value by Jackson and Chiwona-Karltun (2018) discovered that much as more value added products had been processed, the nutritional value had been affected from the use of high cyanogenic glucosides. For consumption safety, the study proposed that more emphasis be placed on identifying cassava varieties with low cyanogenic compounds hence minimizing the toxicity. Also, Panghal, Munezero, Sharma, and Chhikara (2019) explored about the toxicity, detoxifying and culinary uses of cassava. Their exploration revealed that looking at the increased production of cassava and the value of starch in cassava, cassava tuberous roots could be broken down for making starch, syrup, bakery and other products. Since the toxins in cassava restricted its food applications, this study suggested various processing means such as grating, drying, fermentation and boiling for reduced level of toxicity. It also looked at cassava as one of the foods that could ensure food security across the world. The study further advocated for the need to employ modern processing methods to lessen toxins, improve quality so as to meet the world food security needs. Their findings revealed that enhanced cassava production and its starch content, as cassava tuberous roots would be processed to produce starch, syrup, baked goods and other goods. Since the use of cassava was limited by its toxicity, this study suggested various processing means such as grating, drying, fermentation and boiling so as to reduce the level of toxicity. Furthermore, it looked at cassava as one of the foods that can ensure food security across the world. The study further advocated for the need to employ modern processing methods to lessen toxins, improve quality so as to meet the world food

security needs.

Ani et al. (2019) investigated the profitability of cassava processing by providing questionnaires to cassava processors to gather data. Information about the different forms of cassava processing and technology including, cassava chips, dough and flour was collected. The use of either traditional or improved methods was also checked. Analysis was done using the profit function and ANOVA. It revealed that the traditional processing methods were mostly used. The profit margin exploration portrayed that the production of cassava dough, chips and fried cassava granules generates revenue. The results from ANOVA showed that among the three cassava products researched about, fried cassava granules had the highest profit. Much as these processors had challenges like, poor road network, poor equipment, inadequate capital, among others, profit being a key element in any business venture worked as an indicator that determines individual participation.

Research by Tien et al. (2019), on the effects of using wheat flour instead of a mixture of HRCS with vital gluten at 10%, 20% and 30% levels on flour characteristics, bread quality in terms of starch digestibility, and GGI from the resulting bread products. The combined kinds of flours showed reduced viscosities and greater gelatinization temperatures, higher water holding capacities and lower level of expansion than wheat flour. Volumes of bread loaves substituted with HRCS were lower, harder and more sticky. The key finding was that up to 20% of HRCS and essential gluten did not significantly affect bread crumbs, thus it could be used in place of wheat without compromising the bread's quality. A similar case in making bread by Chisenga, Workneh, Bultosa, Alimi, and Siwela (2020) revealed that wheat flour could be replaced with different cassava flour categories to a level of 10% quality of the bread was maintained. Their study further showed that during the baking process, including cassava flour helped to keep more moisture content within the bread which led to a less weight reduction of the final bread product as compared to how it would have been when it was wheat flour used alone.

Production and processing techniques of cassava were investigated by different groups in (Odebode, 2008). Their study showed a significant relationship between cassava varieties grown and the products processed. They hence advocated for the plantation of improved varieties such that more yields would be obtained for both household consumption and industrial use.

Research about crop physiology case history for cassava by Cock and Connor (2021) discovered that much as cassava was once known as a crop used in subsistence farming, it is currently categorised among crops grown on commercial basis like industrial starch products, animal feeds, and fresh food

that is starch based. It led to an increase on the number of cultivators to match the product characteristics and available markets. It was also noticed that due to the increased demand for cassava in both domestic and international markets, there was a high production of cassava since it alleviated famine and had a sustained food supply (Abdul Azeez, 2013). The study on cassava processing and its food application showed that cassava was rich in carbohydrates and consisted of nutrients that were valuable to human health. Therefore, they suggested cassava flour to be the best replacement for wheat, rice and corn flour (Sengar, 2022).

2.2 Major differences between cassava flour and wheat flour

Table 2.1 provides a comprehensive comparison between wheat flour and cassava flour. It aims at highlighting the strengths and weaknesses of each type of flour. This provides a basis for making an informed decision on the kind of flour to be used for baking.

Cassava processing was recognised as a good substitute for wheat flour particularly in developing countries where facing difficulties with the supply of wheat. The CAVA project promoted the use of HQCF, which improved local livelihoods after the employment of better processing techniques. However, challenges such as the presence of toxic compounds in cassava and the need for modern processing methods remained. Over all, cassava production presented a promising opportunity for food security and economic growth (Navacchi et al., 2012).

2.3 Computational Fluid Dynamics in food processing

Different scholars have recognised the role played by CFD in the food processing sector Chhanwal et al. (2012). CFD use in food processing facilities enables products to be handled and kept in more effective systems. It helps food firms to respond to a growing market by improving and developing processing approaches, as well as maintaining high standards for product quality (Norton & Sun, 2006).

In modeling, CFD aided in designing the ovens used for rapid baking, retort processing of tinned liquid, solid foods with an aim of optimizing the process of heat transfer. For baking ovens, it avails details regarding the baking area's air flow pattern and temperature increasing the rate of heat transfer hence enhancing the oven's energy efficiency, decreasing the processing duration and later the final product quality (Anandharamakrishnan & Anandharamakrishnan, 2013; Chhanwal, Moses, & Anandharamakrishnan, 2018).

Table 2.1: Comparison of cassava flour with wheat flour properties.

Parameter	**Cassava Flour**	**Wheat Flour**	**Reference**
Moisture content	Is gluten-free and has different starch properties, making it have lower water absorption	Has high gluten allows content which it to retain more moisture. Its water absorption capacity is higher due to its protein and starch composition	(Li et al., 2023)
Thermal properties	Has different thermal properties due to its unique starch composition. Thermal diffusivity differs significantly which affects the pace at which heat is transferred during baking. This leads to variation in baking time, temperature and moisture profiles	Its properties are greatly influenced by the protein and starch make-up which affect how heat is transferred through the dough	(Oladunmoye et al., 2014)
Rheological properties	Since it's gluten-free, it carries different visco-elastic properties. This affects the ability of the dough to rise and maintain its shape. It brings about the differences in texture of the final product	Presence of gluten in wheat gives it visco-elastic properties which are key for dough formation and its ability to rise and maintain its shape. The elasticity affects how the dough expands and holds shape during baking	(Chisenga et al., 2020)

Using the knowledge of numerical modeling, Moureh and Derens (2000) studied the temperature rise in palletized frozen food across the distribution chain. The study explained the different cases in which frozen food experienced temperature increase. This happened on delivery, loading and offloading procedure. A basic rise in temperature may also take place in case pallets got typically handled in temperature above 0^0C during temporary storage. The study investigated the temperature increase in a pallet through tests and by numerical methods.

Bakeries in the bread industry used ovens that maintained a steady temperature. Due to the configuration of the oven, dough experienced four (4) primary temperature zones during baking. Temperature played the most important role in each zone. Gelatinization, enzymatic processes, and browning reactions were among the mechanisms involved in baking which eventually affected final product's quality. The study by Therdthai, Zhou, and Adamczak (2002) aimed at establishing an ideal temperature range for white sandwich bread which achieved the highest quality of product. A multi-level partial factorial design was used for the experiments, and dough was baked within four (4) evenly spaced temperature zones. To examine how temperature and baking time affect bread quality features, mathematical models were developed. From solving a restrained minimization model, their findings revealed that optimal temperature profile that resulted in the least amount of weight loss was $115^0C, 130^0C, 156^0C, 176^0C$, with a 27.4 minute baking time in each of the zones. The top crust color, side crust color, and averaged crust color were all within an acceptable range, and the crumb temperature was anticipated to reach 99^0C (Therdthai et al., 2002).

The temperature profile and airflow patterns during a continuous industrial baking process were examined using 3-D CFD modeling and simulation techniques by (Therdthai et al., 2004). The established model consisted of moving networks which simulated the characteristics of a continuous commercial baking operation in which dough was transported uninterruptedly inside the oven cavity following a first in, first out arrangement. The model forecasted the dynamic responses during the continuous baking process based on a short-term state assumption. Furthermore, the study explored oven working conditions, such as air flow volume and heat source, which could yield optimal baking conditions. Simulation results indicated that heat supplied was minimized while airflow volume increased, which led to a reduction in the weight loss of the bread.

Research focussing on mathematical modeling of the baking process by Zhang and Datta (2006), showed the relationship between temperature, moisture content, temperature and volume expansion. A model was developed that considered both moisture and heat transport, incorporating the volume change. The model output demonstrated a strong correlation with the experimental findings regarding moisture, temperature, volume alterations, and surface browning. Their findings showed that as temperature increases, moisture content reduces. It also showed that as the baking time increases, the temperature within the dough also increases. The model also revealed that increasing the baking temperature above normal levels decreases the volume of the baked bread. Furthermore, the study found that baking in a microwave tends to heat the bread internally, resulting in a soft crust

and doughy center that caves in.

A CFD model was generated for the bread-baking process in a pilot-scale baking oven by Anishaparvin et al. (2010) to investigate the temperature and starch gelatinization index of bread after hot air distribution and placement of the bread in a given configuration. Product simulation was conducted with different modes of bread placement in the oven, and the results were validated against experimental measurements of bread temperature. The study demonstrated that a non-uniform air flow pattern into the oven chamber leads to uneven temperature distribution. Regarding bread placement, it was found that bread baking on the upper racks experiences shorter baking times and lower gelatinization indices compared to those on the lower racks.

As suggested by Nicolas et al. (2010), a model for bread baking was established using COMSOL Multiphysics, which considered heat and mass transfer coupled with the phenomenon of swelling (expansion). This model predicts temperatures, pressures and water content evolutions in the dough for varied energy requests. The results got were studied according to different physical parameters to clearly understand interactions between the various operations in the porous matrix. Their findings showed that temperature and moisture content evolution were consistent with experimental findings.

Investigation on the bread baking process by Chhanwal, Indrani, Raghavarao, and Anandharamakrishnan (2011) using CFD developed a model to gain knowledge about the temperature and browning profile of bread. The study incorporated the phase shift during evaporation and the mechanism of evaporation-condensation into the baking process model. Bread temperature data obtained experimentally at three distinct locations were used to validate the simulation results. The findings indicated that the crumb temperature never exceeded 100^0C because of the evaporation-condensation mechanism integration into the model. Baking was completed in 25 minutes, as the crumb temperature stabilized at 98^0C.

In conclusion, CFD enhanced the food processing industry by optimizing equipment design, such as baking ovens and improving product quality. It provided critical insights into the temperature and airflow patterns, which were essential for efficient heat transfer. Different scholars highlighted the importance of managing temperature to have the baking conditions optimized through mathematical modeling. Studies have established the optimal temperature profiles for bread baking and revealed how changes in air flow and placement within ovens affected baking outcomes.

2.4 Airflow and temperature distribution

Khatir et al. (2023), used CFD to investigate the airflow and temperature distribution in a small scale bread baking oven. A mathematical model was created and the computed results were verified by comparing them to experimental data gathered within the oven. In their investigation, the oven was operated at various temperatures inside

each zone. The thermal fields inside the oven were then predicted using the CFD model. Authors pointed out that because of the intricacy of the thermal air flows in baking ovens, CFD models needed to be carefully validated before being used for actual oven design. The results demonstrated that precise temperature forecasts were made throughout the oven by carefully choosing the flow model and applying actual boundary conditions.

Research about the temperature profile of a bun during the baking process through CFD modeling under various load conditions Chakraborty and Dash (2023), similar to the work by Tank, Chhanwal, Indrani, and Anandharamakrishnan (2014), these authors investigated the temperature profile of a bun during its baking process using CFD. The model incorporated the consequences of latent heat during water's phase transition, as well as the evaporation and condensation mechanisms, and accurately represented the concrete bun baking process. Simulation and experimental results of bun temperature at two different locations were obtained and validated. The findings showed that the baking process was completed in 20 minutes, and the crumb temperature stabilized at 98^0C. Furthermore, Chhanwal et al. (2012) explored the effect of a partially (two baking trays) loaded and a fully loaded (eight baking trays) oven on the temperature profile of the buns. Findings showed that the profiles of temperature and velocity varied between the fully and partially loaded oven conditions. Additionally, the buns put on the upper racks baked faster, because of the oven's uneven temperature distribution, the lowest rack displayed slower baking. This implied that the placement of the buns in the oven impacts their temperature and, the product's quality.

A mathematical model was generated by Khater and Bahnasawy (2014) to describe the mass balance and heat throughout the baking process. The aim was to forecast the water content and bread temperature under various heating durations and temperatures. The researchers used oven temperatures of 180^0C, 190^0C, 200^0C, 210^0C, and 220^0C in their investigation. The study's findings showed that the temperature of the bread and its weight reduction were directly proportional to the oven temperature. For instance, an increase in the oven temperature from 180^0C to 220^0C led to an increase in the bread temperature from 112.73^0C to 168.49^0C, and a rise in the bread's weight loss from 22.40% to 52.46%. Additionally, the study demonstrated that as baking time increases, oven temperature and weight reduction of the bread also increase. This suggests that both baking time and temperature of the oven have a significant impact on the final temperature and moisture content of the baked bread.

The significance of airflow and temperature distribution was highlighted, where studies found out that proper model selection and validation were crucial for accurate temperature predictions. Factors such as bun placement and oven loading affected baking efficiency and product quality. Increased oven temperature and extended baking times correlated with increased bread temperature and weight loss, which emphasised their impact on the final product.

2.5 Heat and mass transfer

Research about the transfer of heat and mass in industrial biscuit baking ovens was done, focusing on the effect of temperature on baking time was conducted by (Kangarluei, 2015). The findings showed that radiation was the predominant mechanism of heat transfer in the baking process, accounting for 69% of the heat transfer, while convection contributed 28%, and conduction was assumed to be 3%. Additionally, the study revealed that the baking time is directly dependent on the temperature of the baking chamber. For instance, it took 7 minutes for the biscuits to reach a moisture content of 4% when the oven temperature was 200^0C. This suggests that increasing the temperature of the baking chamber can reduce the baking time needed to achieve the desired level of moisture within the final product. In summary, the study highlighted the usefulness of understanding the mechanisms of heat transfer and the relationship between oven temperature and baking time in the industrial biscuit baking process. By using this information, baking conditions may be optimized and production process efficiency can be increased.

According to Cevoli, Panarese, Catalogne, and Fabbri (2020), a numerical model was developed by utilizing the principles of the transfer of mass and heat, which was subsequently inverted to calculate the cake's effective moisture diffusivity while it was baking. The researchers assessed the dependence of diffusivity on both temperature and moisture content. Their findings showed that the inverse method used in the model was able to predict the effective moisture diffusivity during cake baking, and the values obtained approximated to those for similar food products. Additionally, the study discovered that as the oven temperature increases, the moisture concentration within the cake decreases during the baking process. This suggests that higher oven temperatures lead to a faster removal of moisture from the cake, which can impact the final texture and quality of the baked product.

An investigation on the simulation of the bread baking process in an industrial convection oven was made in (Al-Nasser et al., 2021). The researchers aimed at predicting the unsteady multiphase flow, transfer of heat and mass occurring inside the oven, when considering the changes in the bread volume during baking. Since bread contains very small porous openings, the developed model considered the bread's porosity, water evaporation, volume expansion, gelatinization of starch and carbon dioxide emission during the baking process. The numerical solution obtained from the model was validated through experimentation. The predictions from the numerical model, when compared to the experimental findings, showed good agreement. This suggests that the developed simulation effectively captured the complex multiphysics phenomena involved in the industrial-scale bread baking process, including variations in the bread structure and composition during the high-temperature baking conditions.

A study on the simulation of the complex fluid flow patterns exhibited during baking in an oven by Chakraborty et al. (2022), as well as the overall baking process on various bakery products with different raw materials used in the dough formation. The different food materials, each with their unique properties, account for this observed

complexity. In their study, the researchers utilized CFD modeling to project the temperature changes detected inside the oven during the baking process. This approach provides insights that can guide the control of product quality, which is typically the primary aim of any baking process. The study highlights the importance of understanding the impact of raw material properties on the transfer of heat and fluid dynamics phenomena occurring within the oven during baking. By utilizing CFD modeling, the researchers were able to understand the temperature variations inside the oven better, which can be crucial for optimizing the baking conditions and ensuring consistent product quality.

An investigation on the application of CFD to control quality boundaries by profiling the temperature and moisture in baked products was conducted by (Chakraborty & Dash, 2023). The researchers identified temperature as the core aspect in the baking process, as it is a key determinant of the ultimate product's quality and value. The CFD model developed in the study demonstrated its effectiveness in predicting the temperature of the crumb and crust based on the principles of heat transfer. To validate the model's accuracy, the researchers also carried out experiments to measure the transfer mass and heat profiles of the baked products. The justification of the CFD findings was further strengthened by conducting temperature and moisture trials for a specific bakery product using a baking oven. During these experiments, temperature was recorded at 4-5 sections of the product using wireless sensors embedded within the sample. Additionally, the moisture content across all sections was measured by collecting samples and analyzing them in a hot air oven at 105^0C for one day. The experimental records of temperature and moisture were then used to confirm the predictions made by the CFD model. This approach allowed the researchers to validate the CFD estimates and establish the reliability of the computational modeling technique. Furthermore, the study encourages the use of CFD to model the mass distribution, volume growth of different bakery products, as this can provide a more comprehensive understanding of the complex baking process.

Research on the transfer of heat and mass in baking process explained the key role of temperature which influenced baking efficiency and product quality. Studies revealed that radiation was the primary mode of heat transfer while higher temperatures reduced baking time and moisture content levels in cakes and bread. Advanced numerical models and CFD simulations were effectively utilized to capture the complex dynamics such as moisture diffusivity, air flow and temperature distribution changes during baking. These findings point out the importance of understanding the relationship between heat transfer mechanisms and raw material properties.

2.6 Research Gap

A significant research gap exists in the use of CFD techniques specifically for baking with cassava based ingredients. Many studies overlook the unique properties of cassava flour such as moisture content and the presence of toxic compounds which affect baking outcomes. There is need for CFD models that capture the transfer of heat

and mass mechanisms specific for cassava flour in order to control of the baking process.

In conclusion, the literature review highlighted the significance of CFD in industrial processes of value addition, particularly the process of baking. Based on this literature it is highly evidenced that:

1. CFD can effectively optimize the processes involved in cake baking thereby enhancing the quality of the cake product and reducing costs of production.

2. Cassava flour presents new and unique challenges in cake baking process especially the dough texture and structure issues.

3. Indeed, there is limited research at the moment on the use of CFD in food products made fro cassava.

Chapter 3

MATERIALS AND METHODS

The use of CFD in cake baking process with cassava flour as the primary ingredient, this study employs a combination of both mathematical computations and numerical simulation and methodology mainly involved the modification of the existing CFD models and implementation of numerical simulation using CFD software (COMSOL Multiphysics software). This helped with the geometry creation, that is, Cake mold and oven dimensions, mesh generation by use of finite element method, establishment of boundary conditions including temperature, moisture level, and airflow, and simulation parameters for the dough properties, baking time, and temperature.

3.1 Research design

A modified mathematical model was solved using COMSOL Multiphysics software, version 6.2 which employed the Finite Element Method (FEM). The cassava dough was discretized into a computational mesh and set-up within COMSOL Multiphysics covered the geometry and domain configuration, employing initial and boundary conditions, mesh generation strategies and solver format.

3.1.1 The Baking Process

The baking process is a phase in which when exposed to heat, raw dough is changed into crumb and crust texture using an oven or baking chamber as shown in Figure 3.1, Rahman et al. (2021), which is a source of energy, through which heat and mass transfer (Therdthai et al., 2004). Product quality depends on some fluid properties say, temperature, pressure, time, and viscosity (Chhanwal et al., 2012; Anandharamakrishnan & Anandharamakrishnan, 2013).

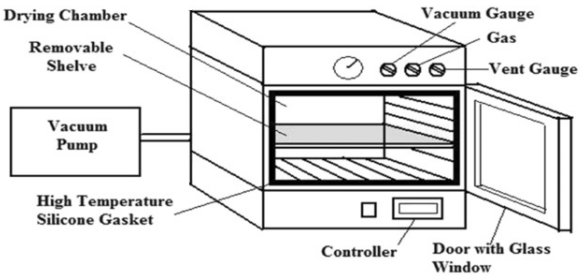

Figure 3.1: An oven baking chamber, adapted from (Rahman et al., 2021)

3.1.2 Description of the Baking Process

Baking is crafted not just to apply heat to items like cakes, bread, biscuits, but also to facilitate the biochemical reactions of the ingredients in the recipe (Zhang & Datta, 2006). The blend of its dry and wet components forms a batter that grants the baked product flexibility enabling it to expand while maintaining its structure (Kianmehr, 1995). Cake baking is a process and in these processes, some assumptions are made and conditions attained. A required quantity of each of the ingredients and additives was measured in the process of making dough. These included; cassava flour, eggs, baking powder, milk, sugar and other flavours.

Tools like ovens or any other source of heat, mixers, dough mixing trough, weighing scale, shaped containers for sizing, chopping board for ingredients to be used Navacchi et al. (2012) and the mathematical model was implemented by using computing and simulation software (package) COMSOL Multiphysics through which equations for heat and mass transmission can be solved. The baking process is characterized by steps or stages as shown in Figure 3.2.

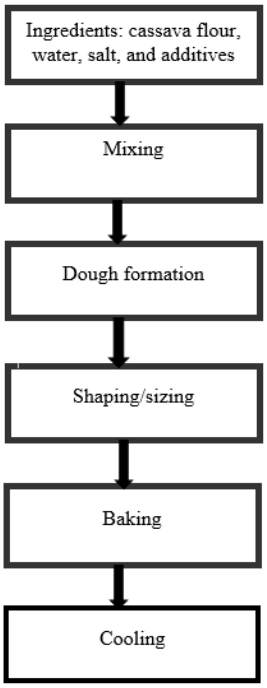

Figure 3.2: Steps involved in the baking process, adopted from (Anandharamakrishnan & Anandharamakrishnan, 2013)

(i) Ingredients: The ingredients in the required proportion of cassava flour, salt, water, lemon, baking powder and other additives comprise of necessary species for the baking process.

(ii) Mixing: The different proportions of ingredients are thoroughly mixed using a mixer until the desired dough texture is achieved.

(iii) Dough Formation: On thorough mixing of all the ingredients with necessary additives, the desired dough is attained. It contains a given mass at a certain temperature, colour, viscosity, smoothness and elasticity.

(iv) Shaping/Sizing: The next stage is deploying at a constant weight, the dough into the baking containers of differing sizes and shapes.

(v) Oven Baking: In the process of oven baking, dough undergoes thermo-physical changes in its shape and composition; that is, density, moisture level and temperature of the dough, the convective mass and heat transfer. The heat transfer process starts at the initial stage of baking, causing a rise in temperature, viscous dissipation and porosity in the dough while the mass transfer process results in moisture loss and release of carbon dioxide leading to swelling or volume expansion (Wong, Zhou, & Hua, 2006). The thermal heat and mass transfer stages involved in oven baking processes are outlined as illustrated in Wong et al. (2006) as in Table 3.1 below:

Table 3.1: Stages of the baking process.

S.No.	**First**	**Second and third**	**Fourth**
1.	CO_2 emitted, loaf volume increased	Maximum: • Evaporation of moisture • Starch gelatinization • Proteins broken down	Volatilization of organic compounds.
2.	Enzyme inactivated (323-333)Kelvin	Produced brown coloured crust	Cell wall firmness.
3.	Yeast/bacteria killed	Caramelization and crust surface	Maillard reaction at at crust surface
4.	Produced thin, expandable, brown coloured skin		Develop desired crust colour.

The detailed description of the stages involved in the baking process as as follows:

(a) Stage One

This begins at a point when dough is placed in an oven. At this stage, the heat and mass transfer process begins. Heat is transferred by radiation, conduction and convection as shown in Figure (3.3).

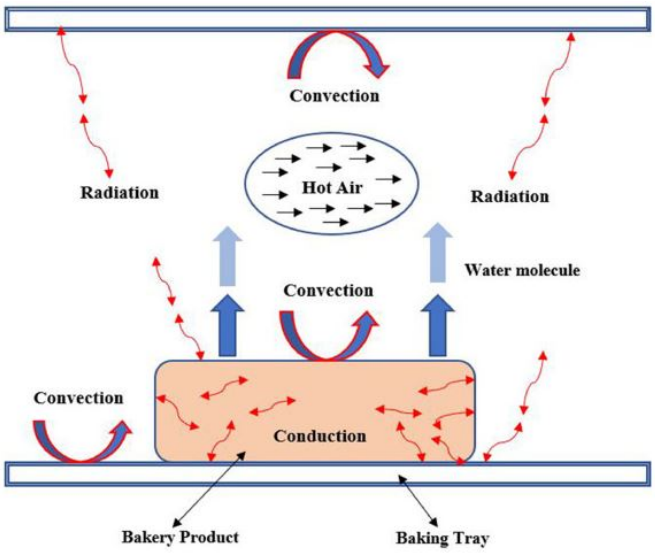

Figure 3.3: Heat Transfer effects within an oven (Chakraborty & Dash, 2023).

The leavening agents such as yeast, baking soda at this stage produce carbon dioxide making an increase in the volume of the bread. As the temperature increases, the yeast is killed. The transfer of heat and mass processes begin at this stage through formation of carbon dioxide (which is formed by the leavening agents in the dough. The yeast changes sugar into carbon dioxide and moisture. This chemical reaction causes the development of pores through which volume expansion occurs). Formation of pores is the process of dough fermentation, yeast produces carbon dioxide which is kept locally in small pores making small volume increment in the dough before baking begins. During baking, a rise in temperature makes more production of carbon dioxide and causes pressure inside the dough to increase. Due to water evaporation, the volume of the pores keeps on increasing (Al-Nasser et al., 2021).

(b) Stages Two and Three

In this stage, solidification and expansion occur due to starch gelatinization (a process of breaking down the inter-molecular bonds of starch molecules in the presence of water and heat). The starch within the dough starts absorbing water which makes the dough to thicken making it more viscous. Protein denaturation (is the process by which when a solution of a protein is boiled, the protein frequently becomes insoluble even when the solution is cooled). As temperature rises, the proteins in the dough are broken down, the denatured proteins are then aggregated together.

Zanoni, Peri, and Bruno (1995) suggested starch gelatinization to be obtained from:

$$\frac{d\alpha}{dt} = K_\alpha(1-\alpha) \tag{3.1}$$

where α represents the degree of gelatinization $(0 \leq \alpha \leq 1)$, K_α stands for reaction rate constant, t is the time(s). Since the rate of reaction, K_α is temperature dependent, it can be obtained from the Arrhenius equation is given by;

$$K_\alpha = K_0 e^{\left(\frac{-E}{RT}\right)}$$

where K_0 is the pre-exponential factor (comes as a result of the frequency at which collisions between fluid molecules take place hence the reaction process), R stands for gas constant, E represents activation energy and T represents temperature in Kelvin.

(c) Stage Four

Reactions from surface browning occur, enhancing colour and flavour. This results from two main reactions, which include maillard reaction and caramelization. Maillard reaction is a chemical reaction between proteins found in the dough and reducing sugars that occurs during the baking process while caramelization is the process where sugars are broken when heated. The two processes contribute to the browning of the surface.

(vi) Cooling; The cooling stage marks the end of the transfer of heat and mass process. It begins immediately after an optimal time of baking is attained through heat loss caused by thermal diffusivity, convection, radiation and evaporation. Radiation, being the primary mode of heat transfer, refers to heat exchange between surfaces at different temperatures without a transfer medium (the oven walls transfer heat to the surface of the product through radiation) which accounts for 50% to 80% of the total heat transfer. Heat transfer through convection takes place from hot air and moisture, while heat transfer through conduction takes place through direct contact between used materials (from the oven baking chamber to the baking container) (Kianmehr, 1995).

Both moisture and heat transfer are affected by the fluid flow characteristics (cooling air temperature, velocity), fluid properties (viscosity, density and conductivity), product surface properties, shape, dimension of the product and physical load placement Hu and Sun (2000). Practically, predicting the cooling time by putting into account all the above factors can be complex and takes longer without using techniques of numerical analysis (Davey & Pham, 1997).

3.1.3 Model Assumptions

The following are the assumptions taken into account during the baking process and model modification (Sadeghi, Hamdami, Shahedi, & Rafe, 2016).

1. The dough is considered to be a multiphase medium, that is, solid (dough), liquid (water), gas (water vapour and Carbon dioxide).

2. Dough is uniform during the baking process. This implies that the mixing of the dough is done thoroughly.

3. The dough is isotropic. This means that the physical properties measured at different points in different directions give the same value. For example, at constant density.

4. Carbon dioxide and water vapour are considered as ideal gases. This implies that even if they mix, they have no effect on the final product.

5. The dough's water content is only eliminated during the baking process by capillary diffusion. It is through the diffusion process that moisture and water vapour formation occur.

6. Mass and energy transfer during the baking process takes place in a single direction.

7. Temperature of hot air is the same as that of the hot surface.

8. Transfer of mass does not occur in regions that are in contact with the hot surface. This means that mass does not move out through the walls of the container being used for baking but rather takes place through open ends where carbon dioxide, moisture and water vapour escape from.

9. Vapour and water transfer within the bread are independent and take place in a multiphase form.

3.1.4 Derivation of Governing Equations

Mathematical modeling of the baking process.

The mathematical model in the baking process is governed by the conservation of mass, conservation of momentum and conservation of energy equations that control fluid flow and heat transfer (Sharma, 2021).

3.1.4.1 Mathematical equation for the law of conservation of mass

The law of conservation of mass states that matter can neither be created nor destroyed (Sharma, 2021). This means that the mass of all reactants should balance with the mass of the final product and moisture lost (Yan & Tu, 2023). The conservation of mass process is governed by the continuity equation which applies to all fluids including; compressible and incompressible fluids, Newtonian and non-Newtonian fluids (White & Majdalani, 2006).

The fluid under consideration will be regarded as a continuum. The conservation laws describe the behaviour of the fluid in terms of microscopic properties such as velocity, pressure, density and temperature as including their space and time derivatives (Chhanwal et al., 2012).

To derive the differential continuity equation, consider a tiny portion of fluid with sides $\triangle x$, $\triangle y$ and $\triangle z$ as shown in Figure 3.4 below. This fluid element is referred to as an infinitesimal control volume Through which the fluid enters and exits. In the xy-plane, the depth is $\triangle z$, in the xz-plane the depth is $\triangle y$ and in the yz-plane, the depth $\triangle x$. For all fluid properties that depend on space and time implies that we have $\rho(x,y,z,t)$, $p(x,y,z,t)$, $T(x,y,z,t)$ and $V(x,y,z,t)$, for density, pressure, temperature and velocity respectively. Since there is a possibility of mass changing inside the element, the mass that flows into the element minus that which flows outside the element should be equal to the change in mass inside the element. Let,

(i) $u = u(x,y,z,t)$ be the inlet velocity component in the x direction,

(ii) $v = v(x,y,z,t)$ be the inlet velocity component in the y direction,

(iii) $w = w(x,y,z,t)$ be the inlet velocity component in the z direction.

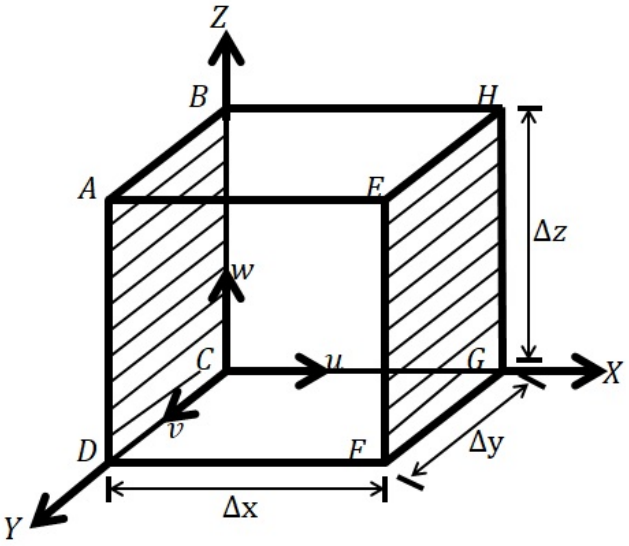

Figure 3.4: Fluid element for conservation laws

(Batchelor, 2000).

Considering fluid mass entering through face ABCD and leaving through face EFGH. The components of the forces acting on the fluid element are as shown in Figure 3.5. Mass of a fluid entering face ABCD per second, is given as,

$$\frac{m}{s} = \rho \times \text{velocity in the } x \text{ direction} \times \text{Area of ABCD}, \tag{3.2}$$

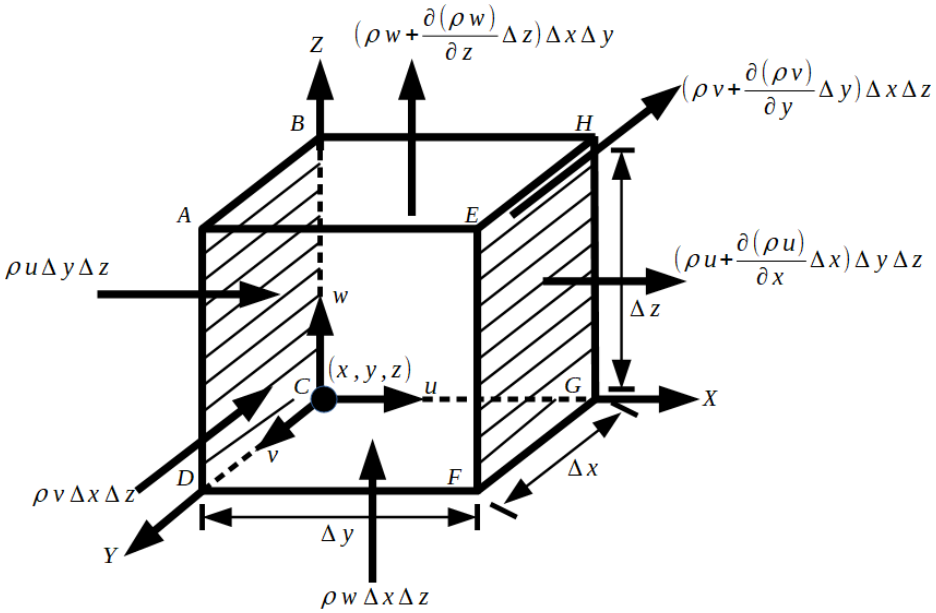

Figure 3.5: Fluid element for showing the forces acting on a fluid element

(White & Majdalani, 2006).

$$= \rho \times u \times (\triangle y \triangle z). \tag{3.3}$$

Mass of the fluid exiting face EFGH per second

$$= \rho u \triangle y \triangle z + \frac{\partial}{\partial x}(\rho u \triangle y \triangle z)\triangle x, \tag{3.4}$$

and rate of increase in mass in the x direction is rate of mass inflow through ABCD - rate of mass outflow through EFGH

$$= \rho u \triangle y \triangle z - \rho u \triangle y \triangle z - \frac{\partial}{\partial x}(\rho u \triangle y \triangle z)\triangle x, \tag{3.5}$$

$$= -\frac{\partial}{\partial x}(\rho u \triangle y \triangle z)\triangle x, \tag{3.6}$$

$$= -\frac{\partial}{\partial x}(\rho u)\triangle x \triangle y \triangle z. \tag{3.7}$$

Similarly, rate of increase in mass in the y direction = $-\frac{\partial}{\partial y}(\rho v)\triangle x \triangle y \triangle z$.

Rate of increase in mass in the z direction = $-\frac{\partial}{\partial z}(\rho w)\triangle x \triangle y \triangle z$.

Total rate of increase in mass = $-(\frac{\partial}{\partial x}(\rho u) + \frac{\partial}{\partial y}(\rho v) + \frac{\partial}{\partial z}(\rho w))\triangle x \triangle y \triangle z$.

Mass of fluid in an element = $\rho(\triangle x \triangle y \triangle z)$.

Rate of increase in mass

$$= \frac{\partial \rho}{\partial t}(\triangle x \triangle y \triangle z). \tag{3.8}$$

Combining equations from (3.3) to (3.8) yield

$$\rho u\triangle y\triangle z-\left(\rho u+\frac{\partial(\rho u)}{\partial x}\triangle x\right)\triangle y\triangle z+\rho v\triangle x\triangle z-\left(\rho v+\frac{\partial(\rho v)}{\partial y}\triangle y\right)\triangle x\triangle z$$
$$+\rho w\triangle x\triangle y-\left(\rho w+\frac{\partial(\rho w)}{\partial z}\triangle z\right)\triangle x\triangle y=\frac{\partial}{\partial t}\left(\rho\triangle x\triangle y\triangle z\right), \tag{3.9}$$

where the density ρ in this case varies across the fluid element. Rearranging the terms in (3.9) and simplifying by dividing through with the term $\triangle x\triangle y\triangle z$, gives

$$\frac{\partial(\rho u)}{\partial x}+\frac{\partial(\rho v)}{\partial y}+\frac{\partial(\rho w)}{\partial z}=-\frac{\partial\rho}{\partial t}. \tag{3.10}$$

By taking derivatives in equation (3.10), gives

$$\frac{\partial\rho}{\partial t}+u\frac{\partial\rho}{\partial x}+v\frac{\partial\rho}{\partial y}+w\frac{\partial\rho}{\partial z}+\rho\left(\frac{\partial u}{\partial y}+\frac{\partial v}{\partial y}+\frac{\partial w}{\partial z}\right)=0. \tag{3.11}$$

The first four terms of equation (3.11) form the material derivative for the density ρ, thus, it can be written as

$$\frac{D\rho}{Dt}+\rho\left(\frac{\partial u}{\partial y}+\frac{\partial v}{\partial y}+\frac{\partial w}{\partial z}\right)=0. \tag{3.12}$$

Therefore, equation (3.12) can also be written as;

$$\frac{D\rho}{Dt}+\rho\,\boldsymbol{\nabla}\cdot\mathbf{V}=0, \tag{3.13}$$

where the velocity $\mathbf{V}=u\mathbf{i}+v\mathbf{j}+w\mathbf{k}$ and the scalar term $\boldsymbol{\nabla}\cdot\mathbf{V}$ is the divergence of the velocity vector.

Considering an incompressible flow, density of a fluid particle remains constant Chakraborty et al. (2022) such that

$$\frac{D\rho}{Dt}=\frac{\partial\rho}{\partial t}+u\frac{\partial\rho}{\partial x}+v\frac{\partial\rho}{\partial y}+w\frac{\partial\rho}{\partial z}=0. \tag{3.14}$$

and at ρ = constant, equation (3.14) reduces to

$$\frac{\partial u}{\partial x}+\frac{\partial v}{\partial y}+\frac{\partial w}{\partial z}=0\quad\text{or}\quad\boldsymbol{\nabla}\cdot\mathbf{V}=0. \tag{3.15}$$

This gives the general form of the equation for conservation of mass.

3.1.4.2 Mathematical equation for the law of conservation of momentum

The law of conservation of momentum (Newton's second law of motion) states that the sum of external forces acting on a fluid particle equals to its rate of change of linear momentum (Tu et al., 2023). It provides an expression describing the relationship between the force applied onto a fluid element, its mass and velocity. The stresses that exist on the faces of an infinitesimal fluid element in a rectangular shape (2 dimensional) are shown in Figure 3.6 (White & Majdalani, 2006). The same components can be extended in the z direction. The normal stresses are denoted by σ and the shear stresses are denoted by τ. The stress components are as follows; σ_{xx}, σ_{yy}, σ_{zz}, τ_{xy}, τ_{yx}, τ_{xz}, τ_{zx}, τ_{yz}, τ_{zy}. When moments are respectively taken about the x-axis, the y-axis and the z-axis, indicate that

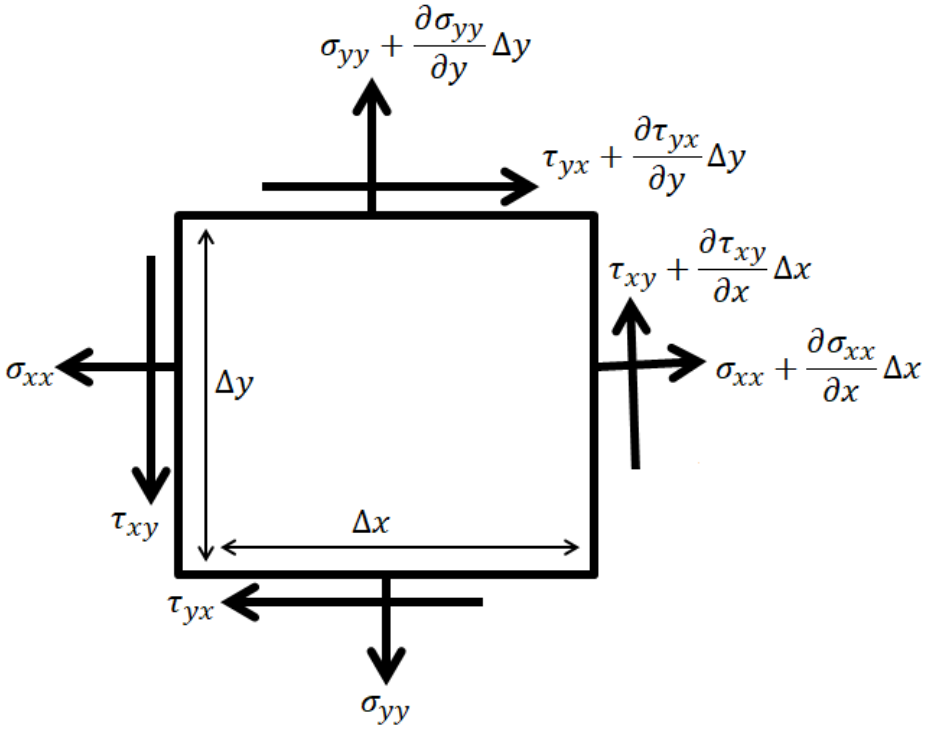

Figure 3.6: Stress components on a fluid element in a 2-D shape

(Batchelor, 2000).

$$\tau_{xy} = \tau_{yx}, \quad \tau_{xz} = \tau_{zx}, \quad \tau_{yz} = \tau_{zy}. \tag{3.16}$$

with six (6) stress components that are related to the pressure p and velocity components u, v and w. Applying Newton's second law to the fluid element in Figure 3.5, which can also be extended to a 3-D geometry, gives

$$F = mg, \tag{3.17}$$

and $(m = \rho V)$

$$\rho V g = F, \tag{3.18}$$

where ρ is the density of the fluid, m is the mass of the fluid, V is the fluid volume, g is the acceleration due to gravity and F is the force acting on the fluid element. Based on Figure 3.5, the effective forces acting on the fluid element in the x direction is given by:

$$\begin{aligned}\rho \triangle x \triangle y \triangle z \frac{Du}{Dt} &= \left(\sigma_{xx} + \frac{\partial \sigma_{xx}}{\partial x}\triangle x\right)\triangle y \triangle z - \sigma_{xx}\triangle y \triangle z \\ &+ \left(\tau_{yx} + \frac{\partial \tau_{yx}}{\partial y}\triangle y\right)\triangle x \triangle z - \tau_{yx}\triangle x \triangle z \\ &+ \left(\tau_{xz} + \frac{\partial \tau_{xz}}{\partial z}\triangle z\right)\triangle x \triangle y - \tau_{xz}\triangle x \triangle y,\end{aligned} \tag{3.19}$$

in the y direction:

$$\begin{aligned}\rho \triangle x \triangle y \triangle z \frac{Dv}{Dt} &= \left(\sigma_{yy} + \frac{\partial \sigma_{yy}}{\partial y}\triangle y\right)\triangle x \triangle z - \sigma_{yy}\triangle x \triangle z \\ &+ \left(\tau_{xy} + \frac{\partial \tau_{xy}}{\partial x}\triangle x\right)\triangle y \triangle z - \tau_{xy}\triangle y \triangle z \\ &+ \left(\tau_{yz} + \frac{\partial \tau_{yz}}{\partial z}\triangle z\right)\triangle x \triangle y - \tau_{yz}\triangle x \triangle y,\end{aligned} \tag{3.20}$$

and z direction:

$$\begin{aligned}\rho \triangle x \triangle y \triangle z \frac{Dw}{Dt} &= \left(\sigma_{zz} + \frac{\partial \sigma_{zz}}{\partial z}\triangle z\right)\triangle x \triangle y - \sigma_{zz}\triangle x \triangle y \\ &+ \left(\tau_{xz} + \frac{\partial \tau_{xz}}{\partial x}\triangle x\right)\triangle y \triangle z - \tau_{xz}\triangle y \triangle z \\ &+ \left(\tau_{yz} + \frac{\partial \tau_{yz}}{\partial y}\triangle y\right)\triangle x \triangle z - \tau_{yz}\triangle x \triangle z - \rho g \triangle x \triangle y \triangle z.\end{aligned} \tag{3.21}$$

From equation (3.19), terms $\sigma_{xx}\triangle y \triangle z$ will be eliminated and then dividing through by $\triangle x \triangle y \triangle z$ gives

$$\rho \frac{Du}{Dt} = \frac{\partial \sigma_{xx}}{\partial x} + \frac{\partial \tau_{yx}}{\partial y} + \frac{\tau_{xz}}{\partial z}. \tag{3.22}$$

From equation (3.20), the terms $\sigma_{yy}\triangle x \triangle z$ will cancel and simplifying further by dividing through with $\triangle x \triangle y \triangle z$ gives

$$\rho \frac{Dv}{Dt} = \frac{\partial \sigma_{yy}}{\partial y} + \frac{\partial \tau_{xy}}{\partial x} + \frac{\tau_{yz}}{\partial z}. \tag{3.23}$$

From equation (3.21), $\sigma_{zz}\triangle x\triangle y$ is eliminated and then dividing through with $\triangle x\triangle y\triangle z$ and gives

$$\rho\frac{Dw}{Dt}=\frac{\partial\sigma_{zz}}{\partial z}+\frac{\partial\tau_{xz}}{\partial x}+\frac{\tau_{yz}}{\partial y}+\rho g. \tag{3.24}$$

Constitutive equations mainly relate the stresses to the velocity and pressure fields. For a newtonian , isotropic fluid (Batchelor, 2000), these stresses have been observed to be;

$$\sigma_{xx}=-p+2\mu\frac{\partial u}{\partial x}+\lambda\boldsymbol{\nabla}\cdot\mathbf{V},\tau_{xy}=\mu\left(\frac{\partial u}{\partial y}+\frac{\partial v}{\partial x}\right), \tag{3.25}$$

$$\sigma_{yy}=-p+2\mu\frac{\partial v}{\partial y}+\lambda\boldsymbol{\nabla}\cdot\mathbf{V},\tau_{xz}=\mu\left(\frac{\partial u}{\partial z}+\frac{\partial w}{\partial x}\right), \tag{3.26}$$

$$\sigma_{zz}=-p+2\mu\frac{\partial w}{\partial z}+\lambda\boldsymbol{\nabla}\cdot\mathbf{V},\tau_{yz}=\mu\left(\frac{\partial v}{\partial z}+\frac{\partial w}{\partial y}\right). \tag{3.27}$$

Substituting equations (3.25), (3.26) and (3.27) into equations (3.22), (3.23) and (3.24) respectively and using $\lambda=-\frac{2}{3}\mu$ (Versteeg & Malalasekera, 1995) where λ is the second coefficient of viscosity. From (3.22),

$$\rho\frac{Du}{Dt}=\frac{\partial\sigma_{xx}}{\partial x}+\frac{\partial\tau_{yx}}{\partial y}+\frac{\partial\tau_{xz}}{\partial z}.$$

First term on the RHS of equation (3.22),

$$\frac{\partial\sigma_{xx}}{\partial x}=\frac{\partial}{\partial x}\left(-p+2\mu\frac{\partial u}{\partial x}+\lambda\boldsymbol{\nabla}\cdot\mathbf{V}\right),$$

$$=\frac{\partial}{\partial x}\left(-p+2\mu\frac{\partial u}{\partial x}+\lambda\left(\frac{\partial u}{\partial x}+\frac{\partial v}{\partial y}+\frac{\partial w}{\partial z}\right)\right),$$

$$=\frac{\partial p}{\partial x}+2\mu\frac{\partial^2 u}{\partial x^2}+\lambda\left(\frac{\partial^2 u}{\partial x^2}+\frac{\partial^2 v}{\partial x\partial y}+\frac{\partial^2 w}{\partial x\partial z}\right),$$

$$=\frac{\partial p}{\partial x}+2\mu\frac{\partial^2 u}{\partial x^2}-\frac{2}{3}\mu\left(\frac{\partial^2 u}{\partial x^2}+\frac{\partial^2 v}{\partial x\partial y}+\frac{\partial^2 w}{\partial x\partial z}\right),$$

$$=-\frac{\partial p}{\partial x}+\mu\frac{\partial^2 u}{\partial x^2}+\mu\frac{\partial^2 u}{\partial x^2}-\frac{2}{3}\mu\frac{\partial^2 u}{\partial x^2}-\frac{2}{3}\mu\frac{\partial^2 v}{\partial x\partial y}-\frac{2}{3}\mu\frac{\partial^2 w}{\partial x\partial z}.$$

Second term on RHS of equation (3.22):

$$\frac{\partial\tau_{yx}}{\partial y}=\frac{\partial}{\partial y}\left(\mu\left(\frac{\partial u}{\partial y}+\frac{\partial v}{\partial x}\right)\right),$$

$$=\mu\left(\frac{\partial^2 u}{\partial y^2}+\frac{\partial^2 v}{\partial y\partial x}\right).$$

Third term on the RHS of equation (3.22):

$$\frac{\partial \tau_{xz}}{\partial z} = \frac{\partial}{\partial z}\left(\mu\left(\frac{\partial u}{\partial z} + \frac{\partial w}{\partial x}\right)\right),$$

$$= \mu\left(\frac{\partial^2 u}{\partial z^2} + \frac{\partial^2 w}{\partial z \partial x}\right).$$

Summing up the results obtained from the first, second and third terms on the RHS of equation (3.22) and equating them to the LHS of (3.22), one obtains

$$\rho\frac{Du}{Dt} = -\frac{\partial p}{\partial x} + \mu\frac{\partial^2 u}{\partial x} + \mu\frac{\partial^2 u}{\partial x} - \frac{2}{3}\mu\frac{\partial^2 u}{\partial x^2} - \frac{2}{3}\mu\frac{\partial^2 v}{\partial x \partial y} - \frac{2}{3}\mu\frac{\partial^2 w}{\partial x \partial z} + \mu\left(\frac{\partial^2 u}{\partial y^2} + \frac{\partial^2 v}{\partial y \partial x}\right) + \mu\left(\frac{\partial^2 u}{\partial z^2} + \frac{\partial^2 w}{\partial z \partial x}\right).$$

After simplifying, one gets;

$$\rho\frac{Du}{Dt} = -\frac{\partial p}{\partial x} + \mu\left(\frac{\partial^2 u}{\partial x^2} + \frac{\partial^2 v}{\partial y^2} + \frac{\partial^2 w}{\partial z^2}\right) + \frac{\mu}{3}\frac{\partial}{\partial x}\left(\frac{\partial u}{\partial x} + \frac{\partial v}{\partial y} + \frac{\partial w}{\partial z}\right). \tag{3.28}$$

Similarly, for equations (3.23) and (3.24), equations (3.29) and (3.30) are obtained, respectively.

$$\rho\frac{Dv}{Dt} = -\frac{\partial p}{\partial y} + \mu\left(\frac{\partial^2 u}{\partial x^2} + \frac{\partial^2 v}{\partial y^2} + \frac{\partial^2 w}{\partial z^2}\right) + \frac{\mu}{3}\frac{\partial}{\partial x}\left(\frac{\partial u}{\partial x} + \frac{\partial v}{\partial y} + \frac{\partial w}{\partial z}\right), \tag{3.29}$$

$$\rho\frac{Dw}{Dt} = -\frac{\partial p}{\partial z} + \mu\left(\frac{\partial^2 u}{\partial x^2} + \frac{\partial^2 v}{\partial y^2} + \frac{\partial^2 w}{\partial z^2}\right) + \frac{\mu}{3}\frac{\partial}{\partial x}\left(\frac{\partial u}{\partial x} + \frac{\partial v}{\partial y} + \frac{\partial w}{\partial z}\right) + \rho g. \tag{3.30}$$

The term ρg is added to represent the gravitational force acting on the fluid element per unit volume. ρg is only added to the equation in the z - direction because gravity acts downwards along the z - axis. While for a homogeneous fluid, $\frac{\partial \mu}{\partial x} = 0$ (White & Majdalani, 2006). For an incompressible fluid flow, $\boldsymbol{\nabla} \cdot \mathbf{V} = 0$, resulting in Navier Stokes equations given as

$$\rho\frac{Du}{Dt} = -\frac{\partial p}{\partial x} + \mu\left(\frac{\partial^2 u}{\partial x^2} + \frac{\partial^2 u}{\partial y^2} + \frac{\partial^2 u}{\partial z^2}\right), \tag{3.31}$$

$$\rho\frac{Dv}{Dt} = -\frac{\partial p}{\partial y} + \mu\left(\frac{\partial^2 v}{\partial x^2} + \frac{\partial^2 v}{\partial y^2} + \frac{\partial^2 v}{\partial z^2}\right), \tag{3.32}$$

$$\rho\frac{Dw}{Dt} = -\frac{\partial p}{\partial z} + \mu\left(\frac{\partial^2 w}{\partial x^2} + \frac{\partial^2 w}{\partial y^2} + \frac{\partial^2 w}{\partial z^2}\right) + \rho g. \tag{3.33}$$

Using the scalar differential operator (Laplacian)

$$\boldsymbol{\nabla}^2 = \frac{\partial^2}{\partial x^2} + \frac{\partial^2}{\partial y^2} + \frac{\partial^2}{\partial z^2}. \tag{3.34}$$

From equations (3.22) to (3.30), the Navier-Stokes equations is

$$\rho \frac{\partial \mathbf{V}}{\partial t} = -\nabla p + \mu \nabla^2 \mathbf{V} + \rho g. \tag{3.35}$$

3.1.4.3 Mathematical equation for the law of conservation of energy

The law of conservation of energy states that energy can neither be created nor destroyed but can be changed from one form to another Yan and Tu (2023), for example from potential energy to kinetic energy and vice-versa. There are 3 forms of energy in a fluid (White & Majdalani, 2006) and these include;

(i) Thermal energy; which is energy obtained from heat supplied to the fluid.

(ii) Kinetic energy; which is defined as energy possessed by the fluid in motion.

(i) Potential energy; which refers to the energy due to a fluid at rest or by its mean position.

The total energy, E, of a fluid is defined as the sum of thermal energy i, kinetic energy $\frac{1}{2}m(u^2+v^2+w^2)$ and gravitational potential energy (Sharma, 2021). In this case, one can include the effects of the potential energy varies as a source term. We define a source term of energy S_E per unit volume which is given by;

$$\rho \frac{DE}{Dt}, \tag{3.36}$$

where $\frac{DE}{Dt}$ is the rate of change in energy. This implies that the quantity of heat energy in the fluid depends on the density of the fluid or mass and the change in energy. The total rate of work done on the fluid particles (which is due to internal forces operating on the fluid particles) surface stresses acting on the particles (Batchelor, 2000) in the x, y, z directions as shown in Figure 3.6 is given by;

$$\begin{aligned}[-div(p\mathbf{u})] + \left[\frac{\partial(u\sigma_{xx})}{\partial x} + \frac{\partial(u\tau_{yx})}{\partial y} + \frac{\partial(u\tau_{zx})}{\partial z}\right] + \left[\frac{\partial(v\tau_{xy})}{\partial x} + \frac{\partial(v\sigma_{yy})}{\partial y} + \frac{\partial(v\tau_{zy})}{\partial z}\right] \\ + \left[\frac{\partial(w\tau_{xz})}{\partial x} + \frac{\partial(w\tau_{yz}}{\partial y} + \frac{\partial(w\sigma_{zz})}{\partial z}\right].\end{aligned} \tag{3.37}$$

where S_E is the source term of energy. Energy in a fluid particle is conserved by equating the rate of change of energy of the fluid particle in Equation (3.36) to the sum of the net rate of work done on the fluid particle in Equation (3.37) and the net rate of increase of energy due to sources (Versteeg & Malalasekera, 1995).

$$\rho\frac{DE}{Dt} = -div(pu) + \left[\left(\frac{\partial(u\sigma_{xx})}{\partial x} + \frac{\partial(u\tau_{yx})}{\partial y} + \frac{\partial(u\tau_{zx})}{\partial z}\right) + \left(\frac{\partial(v\tau_{xy})}{\partial x} + \frac{\partial(v\sigma_{yy})}{\partial y} + \frac{\partial(v\tau_{zy})}{\partial z}\right) + \left(\frac{\partial(w\tau_{xz})}{\partial x} + \frac{\partial(w\tau_{yz})}{\partial y} + \frac{\partial(w\sigma_{zz})}{\partial z}\right)\right] + div(k\ grad\ T) + S_E. \tag{3.38}$$

Equation (3.38) is an energy equation. Extracting out the changes of the kinetic energy during motion of the fluid to obtain an equation for thermal energy (internal energy), i or temperature T.

$$\rho\frac{D\left[\frac{1}{2}(u^2+v^2+w^2)\right]}{Dt} = -u\cdot grad\ p + \left[u\left(\frac{\partial(\sigma_{xx})}{\partial x} + \frac{\partial(\tau_{yx})}{\partial y} + \frac{\partial(\tau_{zx})}{\partial z}\right) + v\left(\frac{\partial(\tau_{xy})}{\partial x} + \frac{\partial(\sigma_{yy})}{\partial y} + \frac{\partial(\tau_{zy})}{\partial z}\right) + w\left(\frac{\partial(\tau_{xz})}{\partial x} + \frac{\partial(\tau_{yz})}{\partial y} + \frac{\partial(\sigma_{zz})}{\partial z}\right)\right] + div(k\ grad\ T) + u\cdot S_E. \tag{3.39}$$

Subtracting Equation (3.39) from Equation (3.38) and defining a new source term as $S_i = S_E - u\cdot S_M$, yields the internal energy equation (3.40)

$$\rho\frac{Di}{Dt} = -p\ div\ u + div\ (k\ grad\ T) + \left[\left(\sigma_{xx}\frac{\partial u}{\partial x} + \tau_{yx}\frac{\partial u}{\partial y} + \tau_{zx}\frac{\partial u}{\partial z}\right) + \left(\tau_{xy}\frac{\partial v}{\partial x} + \sigma_{yy}\frac{\partial v}{\partial y} + \tau_{zy}\frac{\partial v}{\partial z}\right) + \left(\tau_{xz}\frac{\partial w}{\partial x} + \tau_{yz}\frac{\partial w}{\partial y} + \frac{\sigma_{zz}\partial w}{\partial z}\right)\right] + S_i, \tag{3.40}$$

where, $i = c_p\ T$, C_p is the specific heat capacity at constant pressure and $div(u) = 0$. Re-writing equation (3.40) into the temperature equation, gives

$$\rho\ c_p\frac{DT}{Dt} = div\ (k\ grad\ T) + \left[\left(\sigma_{xx}\frac{\partial u}{\partial x} + \tau_{yx}\frac{\partial u}{\partial y} + \tau_{zx}\frac{\partial u}{\partial z}\right) + \left(\tau_{xy}\frac{\partial v}{\partial x} + \sigma_{yy}\frac{\partial v}{\partial y} + \tau_{zy}\frac{\partial v}{\partial z}\right) + \left(\tau_{xz}\frac{\partial w}{\partial x} + \tau_{yz}\frac{\partial w}{\partial y} + \frac{\sigma_{zz}\partial w}{\partial z}\right)\right] + S_i. \tag{3.41}$$

For newtonian fluids, the viscous stresses are proportional to the rate of deformation (Kapur, 2023). The three dimensional form of the Newtonian law of viscosity for compressible flows has two constants of proportionality namely: dynamic viscosity, μ, which relates to stresses to linear deformation, and second viscosity, λ, which relates stresses to volumetric deformation. The nine viscous stress components (Batchelor, 2000) of which six are

independent include:

$$\sigma_{xx} = 2\mu\frac{\partial u}{\partial x} + \lambda\ div\ u,$$

$$\sigma_{yy} = 2\mu\frac{\partial v}{\partial y} + \lambda\ div\ u,$$

$$\sigma_{zz} = 2\mu\frac{\partial w}{\partial z} + \lambda\ div\ u,$$

$$\tau_{xy} = \tau_{yx} = \mu\left(\frac{\partial u}{\partial y} + \frac{\partial v}{\partial x}\right), \tag{3.42}$$

$$\tau_{xz} = \tau_{zx} = \mu\left(\frac{\partial u}{\partial z} + \frac{\partial w}{\partial x}\right),$$

$$\tau_{yz} = \tau_{zy} = \mu\left(\frac{\partial v}{\partial z} + \frac{\partial w}{\partial y}\right).$$

Liquids are incompressible, so the conservation equation of $div\ \mathbf{u} = 0$ and the viscous stresses are just twice the local rate of linear deformation multiplied by the dynamic viscosity (Versteeg & Malalasekera, 1995).

$$\rho\frac{Di}{Dt} = -p\ div\ u + div\ (k\ grad\ T) + \phi + S_i. \tag{3.43}$$

The effects due to viscous stresses in this internal energy equation are described by the dissipation function which is equal to;

$$\phi = \mu\left\{2\left[\left(\frac{\partial u}{\partial x}\right)^2 + \left(\frac{\partial v}{\partial y}\right)^2 + \left(\frac{\partial w}{\partial z}\right)^2\right] + \left[\left(\frac{\partial u}{\partial y} + \frac{\partial v}{\partial x}\right)^2 + \left(\frac{\partial u}{\partial z} + \frac{\partial w}{\partial x}\right)^2 + \left(\frac{\partial v}{\partial z} + \frac{\partial w}{\partial y}\right)^2\right]\right\}$$
$$+ \lambda(div\ u)^2. \tag{3.44}$$

Hence, the energy equation becomes;

$$\rho C_p\frac{\partial T}{\partial t} + \rho C_p v\nabla T = \nabla\cdot(\lambda\nabla T) \tag{3.45}$$

From equations (3.13), (3.35) and (3.45), we have;

$$\frac{D\rho}{Dt} + \rho\ \boldsymbol{\nabla}\cdot\mathbf{V} = 0, \tag{3.46}$$

$$\rho\frac{\partial \mathbf{V}}{\partial t} = -\nabla p + \mu\nabla^2\mathbf{V} + \rho g, \tag{3.47}$$

$$\rho C_p\frac{\partial T}{\partial t} + \rho C_p v\nabla T = \nabla\cdot(\lambda\nabla T). \tag{3.48}$$

3.1.5 Mathematical Model Modification

From equation (3.13), the following can be deduced;

Equation for mass conservation of the solid is;

$$\frac{\partial \rho_s}{\partial t} + \nabla \cdot (\rho_s v_s) = 0, \tag{3.49}$$

where v_s is the deformation velocity (ms^{-1}), ρ_s is the density of the solid (cassava dough) (Kgm^{-3}). Equation for mass conservation of the liquid (water) is given as;

$$\frac{\partial \rho_l}{\partial t} + \nabla \cdot (\rho_l v_s) = -\nabla \cdot n_1 - G_w, \tag{3.50}$$

where ρ_l represents density of the liquid (water) (Kgm^{-3}), n_1 is the species flow for the liquid (water) $(Kgm^{-2}s^{-1})$, G_w is the consumption rate of water $(Kgm^{-3}s^{-1})$. Equation for mass conservation of the vapour (water) is given as;

$$\frac{\partial \rho_v}{\partial t} + \nabla \cdot (\rho_v v_s) = -\nabla \cdot n_2 + G_w, \tag{3.51}$$

where ρ_v stands for density of the water vapour (Kgm^{-3}), ρ_l represents density of the liquid (water) (Kgm^{-3}), n_2 is the species flow for vapour) $(Kgm^{-2}s^{-1})$, G_w generation rate of vapour $(Kgm^{-3}s^{-1})$. Equation for mass conservation of carbon dioxide is given as;

$$\frac{\partial \rho_c}{\partial t} + \nabla \cdot (\rho_c v_s) = -\nabla \cdot n_3 + G_c, \tag{3.52}$$

where ρ_c is the density of carbon dioxide (Kgm^{-3}), n_3 is the species flow for carbon dioxide $(Kgm^{-2}s^{-1})$, G_c is the generation rate of carbon dioxide $Kgm^{-3}s^{-1}$.

Adding equations (3.49), (3.50) and (3.51) yields,

$$\frac{\partial}{\partial t}(\rho_s + \rho_l + \rho_v) + \nabla \cdot (v_s(\rho_s + \rho_l + \rho_v)) = -\nabla \cdot n_1 - \nabla \cdot n_2, \tag{3.53}$$

where n_i : species flow for $i = 1,2,3$ such that n_1 is the species flow for the liquid by Fick's law; n_2 : species flow for vapour by Darcy's law and n_3 : species flow for carbon dioxide.

But moisture content, W, is the ratio of the mass of water (liquid and vapour) to dry mass (Nicolas et al., 2010).

$$W = \frac{\rho_l V_l + \rho_v V_v}{\rho_s V_s}, \tag{3.54}$$

where V_l, V_v and V_s are the volumes of the liquid, vapour and solid dough respectively. Implying that,

$$W\rho_s V_s = \rho_l V_l + \rho_v V_v. \tag{3.55}$$

Substituting equation (3.55) into (3.53) yields,

$$\begin{aligned} &\frac{\partial}{\partial t}\left(\frac{\rho_l V_l + \rho_v V_v}{W V_s} + \frac{W\rho_s V_s - \rho_v V_v}{V_l} + \frac{W\rho_s V_s - \rho_l V_l}{V_v}\right) \\ &\qquad + \nabla \cdot v_s \left(\frac{\rho_l V_l + \rho_v V_v}{W V_s} + \frac{W\rho_s V_s - \rho_v V_v}{V_l} + \frac{W\rho_s V_s - \rho_l V_l}{V_v}\right) \\ &\qquad = \quad -\nabla \cdot n_1 - \nabla \cdot n_2, \end{aligned} \tag{3.56}$$

$$\begin{aligned} &\frac{\partial}{\partial t}\left(\frac{\rho_l V_l + \rho_v V_v}{W V_s} + \frac{W\rho_s V_s - \rho_v V_v}{V_l} + \frac{W\rho_s V_s - \rho_l V_l}{V_v}\right) \\ &\qquad + \nabla \cdot v_s \left(\frac{\rho_l V_l + \rho_v V_v}{W V_s} + \frac{W\rho_s V_s - \rho_v V_v}{V_l} + \frac{W\rho_s V_s - \rho_l V_l}{V_v}\right) \\ &\qquad = \quad -\nabla \cdot (n_1 + n_2). \end{aligned} \tag{3.57}$$

Equation (3.57) is the equation for the moisture content.

By Fick's law, the species flow n_1 can be expressed as;

$$n_1 = D_l^W \nabla W, \tag{3.58}$$

where D_l^W is the diffusion coefficient for the liquid phase and is obtained from (Zhang & Datta, 2006).

$$D_l^W = -10^{-6} exp(-10 + 10W)\varepsilon, \tag{3.59}$$

where ε is porosity.

Also, by Darcy's law, the species flow, n_2 is calculated from (Cutté, Le Bideau, Glouannec, & Le Page, 2016)

$$n_2 = D_v^T \Delta T + D_v^W \Delta W + D_v^\rho \Delta p, \tag{3.60}$$

where p - pressure due to the gas.

Substituting equations (3.58) and (3.60) into (3.57), we obtain the moisture content transport equation.

$$\begin{aligned}\frac{\partial}{\partial t}\left(\frac{\rho_l V_l+\rho_v V_v}{WV_s}+\frac{W\rho_s V_s-\rho_v V_v}{V_l}+\frac{W\rho_s V_s-\rho_l V_l}{V_v}\right)&\\ +\nabla\cdot v_s\left(\frac{\rho_l V_l+\rho_v V_v}{WV_s}+\frac{W\rho_s V_s-\rho_v V_v}{V_l}+\frac{W\rho_s V_s-\rho_l V_l}{V_v}\right)&\\ = \quad -\nabla\cdot(D_l^W\nabla W+D_v^T\Delta T+D_v^W\Delta W+D_v^\rho\Delta p).&\end{aligned}$$

The total pressure within the dough can be obtained from (Bárcenas, Altamirano-Fortoul, & Rosell, 2010);

$$K_T\frac{\partial T}{\partial t}+K_W\frac{\partial W}{\partial t}+K_p\frac{\partial p}{\partial t}+K_\varepsilon\frac{\partial \varepsilon}{\partial t}+\nabla\cdot(v_s\rho_c)=-\nabla\cdot(D_c^T\Delta T+D_c^W\Delta W+D_c^p\Delta p)+G_c, \tag{3.61}$$

where K_T is the coefficient representing the influence of temperature on the mass balance, K_W is the coefficient representing the influence of moisture content on the mass balance, K_p is the coefficient representing the influence of gas pressure on the mass balance and K_ε is the coefficient representing the influence of porosity on the mass balance.

The porosity, ε is obtained from (Al-Nasser et al., 2021),

$$-\rho_s\frac{\partial \varepsilon}{\partial t}+\nabla\cdot(v_s(1-\varepsilon)\rho_s)=0, \tag{3.62}$$

Modification of the energy equation (3.45) to phase change $\triangle K$ and latent heat of vaporization L_v as;

$$\rho\ C_p\frac{\partial T}{\partial t}+\nabla\cdot(\rho c_p\ v_s T)=-\nabla\cdot(k\nabla T)-\triangle K L_v, \tag{3.63}$$

This was based on the fact that there will be transitions from one phase to another (from liquid to gas) depending on the temperature. While the latent heat of vaporization explains how energy is conserved during phase transitions showing the transformation of energy during the baking process. But;

$$KL_v=n_1h_l+n_2h_v+n_3h_c, \tag{3.64}$$

where h is the enthalpy, with $h_l=c_{pl}(T-T_0)$, $h_v=c_{pv}(T-T_0)$, and $h_c=c_{pc}(T-T_0)$. Hence,

$$KL_v=D_l^W\nabla W\ c_{pl}(T-T_0)+(D_v^T\Delta T+D_v^w\Delta w+D_v^\rho\Delta P)\ c_{pv}(T-T_0)+(D_c^T\Delta T+D_c^W\Delta W+D_c^p\Delta p)\ c_{pc}(T-T_0). \tag{3.65}$$

where T_0 is the initial temperature.

A viscoelastic model was used to predict the swelling of the dough due to the increase in the total gas pressure.

From Kelvin-Voigt model (Zhang & Datta, 2006),

$$\nabla \cdot \sigma = \nabla p, \tag{3.66}$$

where

$$\sigma = 2\mu\varepsilon$$

with

$$\varepsilon = \frac{1}{2}\left[(\nabla\, v_s)^T + \nabla\, v_s\right]$$

.

3.1.6 System of summarised model equations to be solves numerically

Equation for moisture content is,

$$\begin{aligned}\frac{\partial}{\partial t}\left(\frac{\rho_l V_l + \rho_v V_v}{W V_s} + \frac{W\rho_s V_s - \rho_v V_v}{V_l} + \frac{W\rho_s V_s - \rho_l V_l}{V_v}\right) & \\ + \nabla \cdot v_s\left(\frac{\rho_l V_l + \rho_v V_v}{W V_s} + \frac{W\rho_s V_s - \rho_v V_v}{V_l} + \frac{W\rho_s V_s - \rho_l V_l}{V_v}\right) & \\ = \quad -\nabla \cdot (D_l^W \nabla W + D_v^T \Delta T + D_v^W \Delta W + D_v^\rho \Delta p). &\end{aligned}$$

Equation of mass for conservation of carbon dioxide is given as;

$$\frac{\partial \rho_c}{\partial t} + \nabla \cdot (\rho_c v_s) = -\nabla \cdot n_3 + G_c \tag{3.67}$$

For the Energy equation,

$$\rho\ c_p \frac{\partial T}{\partial t} + \nabla \cdot (\rho c_p\ v_s T) = -\nabla \cdot (k\nabla T) - dKL_v$$

Equation for porosity is;

$$-\rho_s \frac{\partial \varepsilon}{\partial t} + \nabla \cdot (v_s(1-\varepsilon)\rho_s) = 0$$

Viscoelastic model based on Kelvin-Voigt model is given by

$$\nabla \cdot \sigma = \nabla p$$

3.1.7 Initial conditions and boundary Conditions

Initial and boundary conditions in CFD are key parameters which state the starting state of a system and constraints at the boundaries of the domain for accurate simulations since this study deals with PDEs.

3.1.7.1 Moisture content equation.

Air/dough interface:

Evaporation of water occurs at the surface of the cake. So, M_w is based on the difference between the partial vapour pressure between the surface of the cake and that of the hot air.

$-n(n_1+n_2) = \frac{k_m M}{R}(\frac{p_{v,surf}}{T} - \frac{p_{v,\infty}}{T_\infty}) = m_w$

where p_v is the vapour pressure (Pa), K_m is the mass transfer coefficient (ms^{-1}) and m_w is the water evaporation rate $Kgm^{-2}s^{-1}$

Mold/dough interface:

In this case, a zero mass flux condition is put into account. $-n(n_1+n_2) = 0$

3.1.7.2 Energy equation.

Air/dough interface:

Heat is shifted to the cake surface by convection and radiation, and balanced by conduction.

$-K\ \nabla\ T = h(T_\infty - T) + \varepsilon\sigma(T_{oven}^4 - T^4) - n_1 L_v$

Mold/dough interface:

$-n(-k_{eff}\nabla T) = -n(-k_{mold}\nabla T_{mold})\ T = T_{mold}$

3.1.7.3 Gas pressure equation.

Total gas pressure is assumed to be constant, equal to atmospheric pressure.

$p_g = p_{atm}$

3.1.7.4 Visco-elastic Model.

$\sigma = 0$, $-n(v_s\ \rho_s) = 0$

3.1.8 Initial Conditions

Initial temperature, $T_0 = 293K$

Initial moisture content = 0.68 $KgKg^{-1}$

Density of cassava flour = 1490.07 Kgm^{-3}

Specific heat capacity = 1827.71 $JKg^{-1}K^{-1}$

Thermal conductivity of cassava flour = 0.27$Wm^{-1}\ ^{0}C^{-1}$

Diffusivity = 9.64 $\times 10^{-4} m^2 s^{-1}$

The above initial conditions are captured from (Mwape et al., 2023). Fixed values are set at the boundaries of the domain for variables like moisture content, temperature, density of the cassava dough. The fluxes or gradients of heat, pressure across the boundaries.

3.1.9 Model and Computational domain

The domain refers to the region where fluid flow and its properties are studied. It also entails the boundaries within which the fluid flow behaviour is analysed including the geometry of the system under study. The geometry set up of the structure of an oven and the cake is developed using SpaceClaim software. The various parts of the oven are made of different materials which include; the oven door which is made out of glass, the upper coils are made up of Copper, the overall outer surface and baking racks are made of Aluminium. Inside the oven, on the top rack is a cake placed on the cake plate.

3.1.10 Non Meshed 3-D Geometry of the Baking Oven

Figures 3.7 (a) and (b) illustrates the outer surface of the baking oven and the inner surface chambers of the baking oven with the cake sitted on a plate respectively.

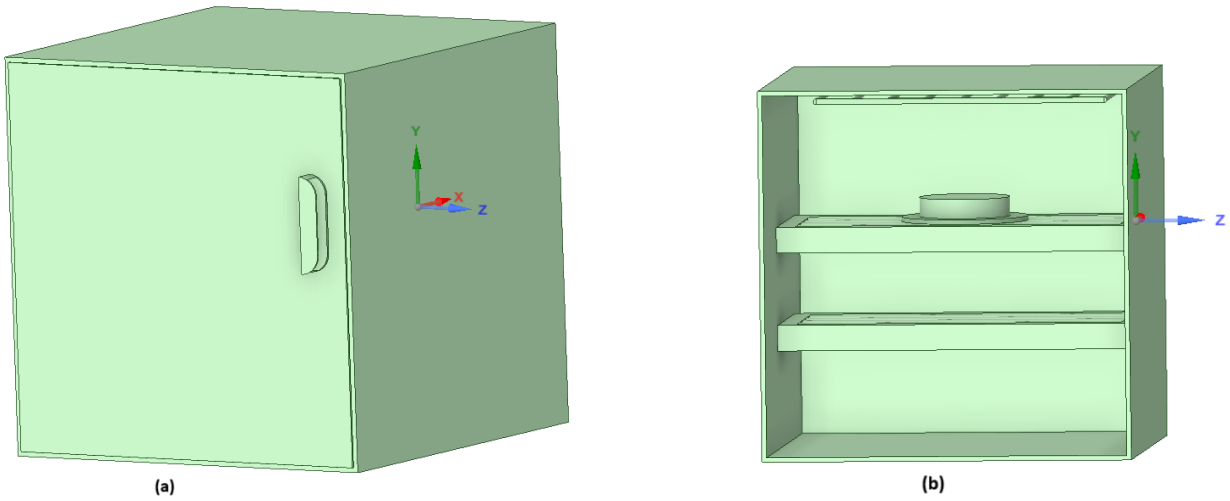

Figure 3.7: The 3-D geometric illustration of the enclosed (a), inner surface chambers of the baking oven in (b).

Because of the complexity of working with a 3-D model, the model was reduced to a 2-D to improve the

computational efficiency. This simplification also takes care of the key aspects considered in the baking process without compromising on the accuracy of the solution. The set-up of the structure of the cake dough was developed using SpaceClaim software.

3.1.11 General structure

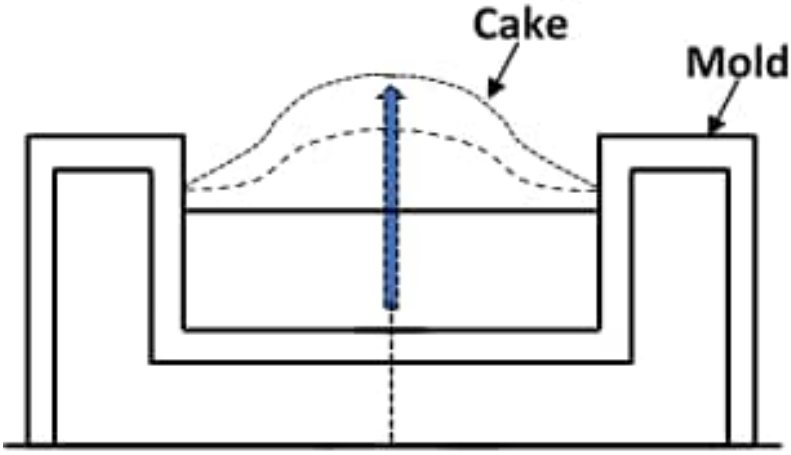

Figure 3.8: General structure of the dough illustrating its expansion in height

Figure 3.8, illustrates the dough placed in a trough of rectangular case before baking starts.

3.1.11.1 Mesh Generation

Meshing is one of the critical steps used in CFD. It involves breaking down of the domain into smaller elements or cells. The elements made form a grid structure which corresponds to the geometry of the domain. This enables any complex fluid behaviour to be analysed using numerical methods. The several non conformable cells make the mesh finer which contributes to the accuracy and consistency of the solution. Meshing is vital as it dictates how well the fluid flow behaviour is depicted within the computational space (Lintermann, 2021). After the meshing process is completed, the next step is solving the governing equations of fluid flow within individual mesh elements using numerical techniques (Tank et al., 2014). Meshing and numerical solving are interdependent in a way that the characteristics of the grid structure generated has an effect on the accuracy and stability of the numerical solution obtained (Sharma, 2021).

3.1.12 Determination of the temperature and moisture content profiles.

The moisture content and temperature of the cake during the baking process are obtained from subjecting the modified system of governing equations together with the initial and boundary conditions to COMSOL Multiphysics

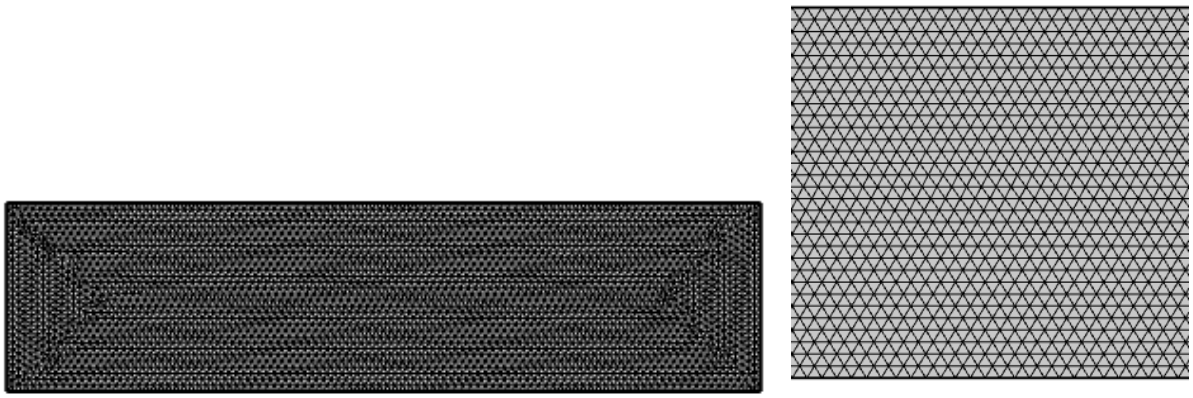

Figure 3.9: Structure of the meshed dough - zoomed structure of the meshed dough

software in the presence of the meshed dough (domain). The software solves the system of equations for each of the cells formed on the meshed dough. It then gives the behaviour of the fluid in different forms; vector plots (graphs), contours.

3.1.12.1 Computational Fluid Dynamics.

CFD codes are designed around the numerical systems (algorithm) which handle problems concerning fluid flow. All codes consist of three main elements which include;

(a) pre-processor

(b) a solver

(c) a post-processor

(a) Pre-processor

This consists of the input of a flow problem to a given CFD problem by using an operator friendly interface. Pre-processing involves activities like;

(i) Definition of the flow geometry

(ii) Grid generation. This involves dividing the domain into smaller sub-sections to form a grid (mesh) which consists of cells that form control volumes or elements.

(iii) Definition of the fluid properties.

(iv) Description of the boundary conditions at the cells along the domain (fluid surface)

The accuracy of a CFD solution is governed by the number of cells in a grid. The more the number of cells in a grid, the finer the mesh and the more accurate the solution.

(b) Solver

There are three different classes of numerical solution techniques namely; finite difference, finite element and finite volume methods. The above numerical methods are used in the following as in (Sharma, 2021)

(i) Approximation of unknown flow variables by means of simple functions.

(ii) Discretization by substitutions into the governing flow equations.

(iii) Aid in obtaining the solution to the algebraic equations.

The key alterations between the above numerical techniques are linked to the way in which the flow variables are approximated and with the discretization methods.

(c) Post-processor

This is concerned with the final produce (solution) to the fluid problem. With the different capacities of the different CFD packages, the following can be viewed at this stage.

(i) Domain geometry and grid display.

(ii) Vector plots.

(iii) Particle tracking.

CFD consists of 3 main steps namely; discretization, obtaining a solution to the discretized equations and post processing (Tu et al., 2023).

Discretization refers to the breaking down of huge volume of a fluid into smaller volumes (Sharma, 2021). It is one of the most important steps in CFD. The problem should be discretized optimally in order to obtain good results. When the domain has been meshed and the linear algebraic equations are formed, solving comes in next. The computer solves the problem in iterations. In case the discretization is done well, the computer solves without finding any challenges, one gets a solution that converges (the solution obtained is approximated to the real solution of the differential equations).

3.1.13 Determining the optimal conditions

The optimal conditions for baking were obtained from making comparisons basing on the results got from the second objective. The graphs of rate of change in temperature, moisture content variation with baking time and expansion in height variation with baking time are utilised in this case.

In conclusion, the study successfully employed a combination of mathematical models and numerical simulation to investigate the application of CFD in the cake baking process using cassava flour.

Chapter 4

RESULTS AND DISCUSSION

This chapter uses the system of equations for baking that accounts for the moisture, carbon dioxide, energy, porosity and visco-elasticity together with boundary conditions to obtain the numerical simulations using COMSOL Multiphysics software. These portray the temperature distribution and mousture content profiles throughout the baking process. Cassava cake expansion is also considered.

4.1 Results on Model modification

The existing models on baking were modified to incorporate the effects of moisture, carbon dioxide, porosity, energy and visco-elasticity.

Equation for moisture content is,

$$\begin{aligned}\frac{\partial}{\partial t}\left(\frac{\rho_l V_l+\rho_v V_v}{WV_s}+\frac{W\rho_s V_s-\rho_v V_v}{V_l}+\frac{W\rho_s V_s-\rho_l V_l}{V_v}\right)&\\ +\nabla\cdot v_s\left(\frac{\rho_l V_l+\rho_v V_v}{WV_s}+\frac{W\rho_s V_s-\rho_v V_v}{V_l}+\frac{W\rho_s V_s-\rho_l V_l}{V_v}\right)&\\ = \quad -\nabla\cdot(D_l^W\nabla W+D_v^T\Delta T+D_v^W\Delta W+D_v^\rho\Delta p).&\end{aligned}$$

Equation of mass for conservation of carbon dioxide is given as;

$$\frac{\partial \rho_c}{\partial t}+\nabla\cdot(\rho_c v_s)=-\nabla\cdot n_3+G_c \tag{4.1}$$

For the Energy equation,

$$\rho\ c_p\frac{\partial T}{\partial t}+\nabla\cdot(\rho c_p\ v_s T)=-\nabla\cdot(k\nabla T)-dKL_v$$

Equation for porosity is;

$$-\rho_s\frac{\partial \varepsilon}{\partial t}+\nabla\cdot(v_s(1-\varepsilon)\rho_s)=0$$

Equation for predicting the swelling of the dough (Viscoelastic model) based on Kelvin-Voigt model is given by

$$\nabla\cdot\sigma=\nabla p$$

4.2 Numerical Simulations

A computer calculation carried out in accordance with a software that applies a mathematical model for a physical system is known as a numerical simulation (Tu et al., 2023). In this study, the simulations were done using COMSOL Multiphysics software.

4.2.1 Results on temperature distribution profiles

During the baking process, temperature distribution within the dough keeps on varying with baking time. This study illustrates it at time t = 0, t = 15, t = 30 and t = 45 minutes. As more heat is dissipated in the baking chamber, the temperature inside the dough begins rising. This was also portrayed by (Al-Nasser et al., 2021). This is also showed by the temperature contours at times t=0, t=15, 30 and 45 minutes respectively. Initially, at $t = 0$ minutes,

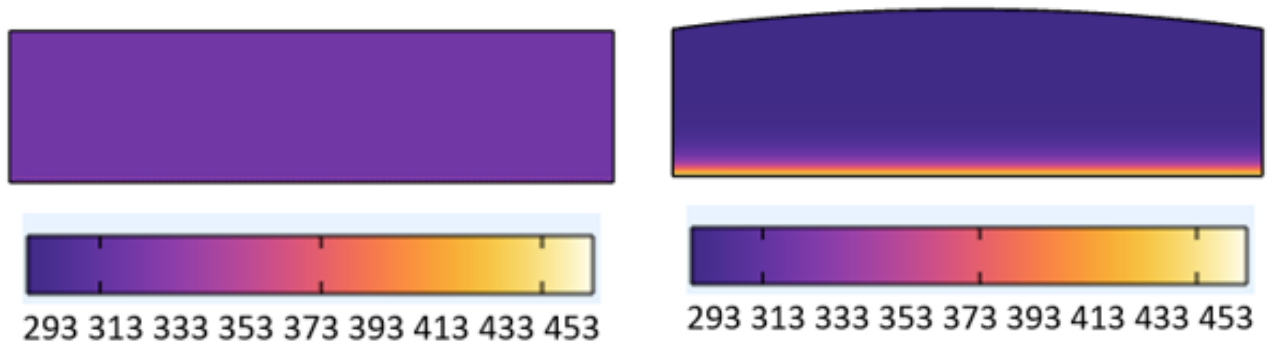

Figure 4.1: Temperature at (t=0 mins) Temperature at (t=15 mins)

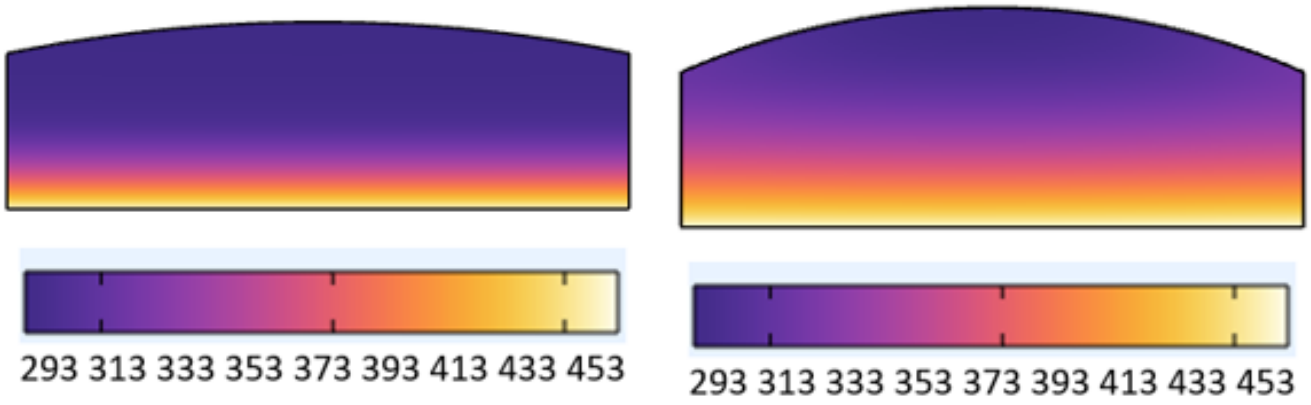

Figure 4.2: Temperature at (t=30 mins) Temperature at (t=45 mins)

there is a uniform temperature distribution throughout the dough which is shown by the solid purple colour. This is because the dough has not yet been subjected to any source of heat.

After 15 minutes, there is an increase in the temperature of the dough which comes as a result of heat supply from the oven or any other heat source. As temperature rises, a series of processes like gelatinization of starch, denaturation of proteins, leavening and moisture evaporation begin to take place. But at this level, they occur at a slower rate.

At $t = 30$ minutes, temperature is higher since it increases with time, implying a faster rate at which the physical and chemical processes occur during the baking process. This reflects a higher rate of moisture evaporation, protein coagulation and production of carbon dioxide which causes volume expansion.

Between $t = 30$ and $t = 45$ minutes, the temperature increases, this means that there is more moisture loss, faster rate of leavening which brings about more carbon dioxide production which cause dough expansion. Beyond 45 minutes, there is no more cake expansion implying that increasing baking time and temperature will affect the end product since all the baking stages have already been completed. Close to the final stages of the baking process, the surface of the dough is subjected to intense heat of the oven leading to the formation of a crust. The crust formed hinders moisture loss. In other words, at this stage, moisture is closed in the cake.

Following Zhang and Datta (2006); Cevoli et al. (2020); Cutté et al. (2016) as baking time increases, it implies that there is still more heat supplied from the oven causing the temperature within the dough to also increase as shown in Figure 4.3 below.

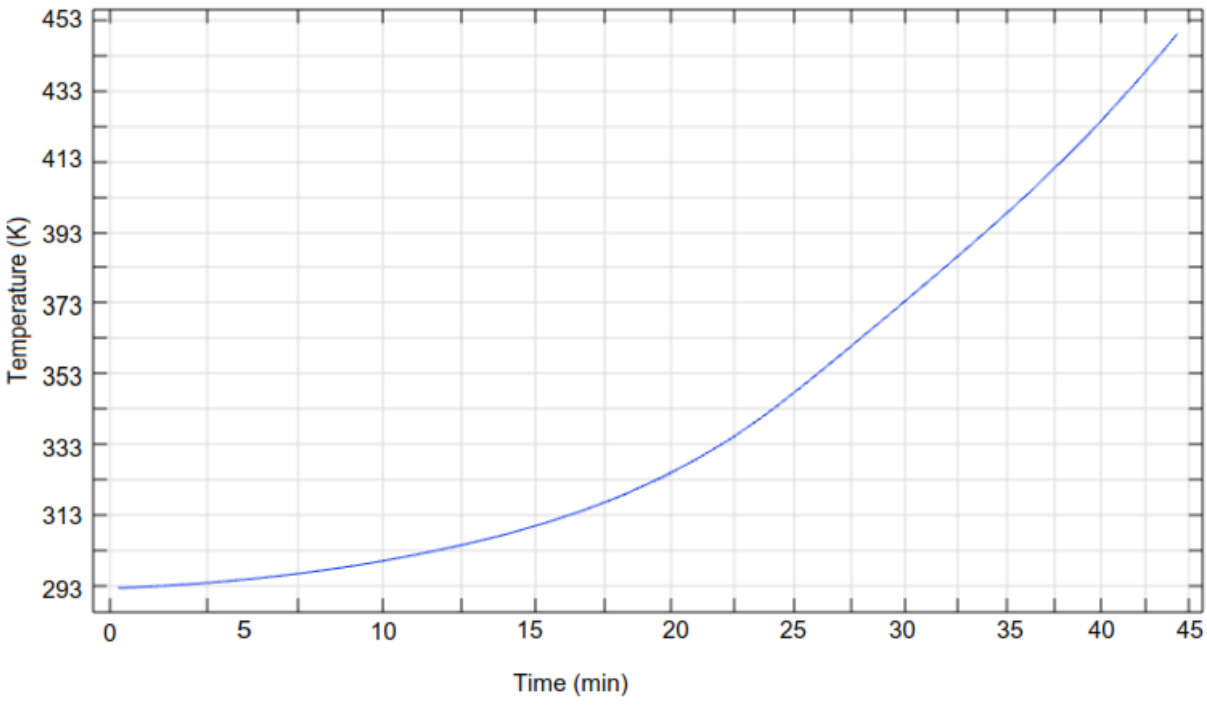

Figure 4.3: A graph of temperature inside the cassava cake against time.

The graph below shows that temperature increases with time. It also indicates no fluctuations in temperature

which shows that cake baking is uniform. The gradual increase in temperature reflects a gradual change of the dough into a baked cake.

In general, the graph provides vital information on how the cake responds to heat during the baking process showing the usefulness of temperature control in order to achieve a quality cake.

In summary, temperature is a key element in the baking process since it influences different physiochemical changes that are the basis of the final texture, flavour and structure of any baked product.

4.2.2 Moisture content profiles

The moisture content scales in ascending order across the gradient as shown by the colour changes from blue to red. (Red indicates a higher moisture content while blue indicates a lower moisture content level). As the colour gradient transitions from blue to red, it shows an increase in temperature gradient. The middle colours like cyan, green, yellow and orange reflect varying levels of moisture content as temperature changes.

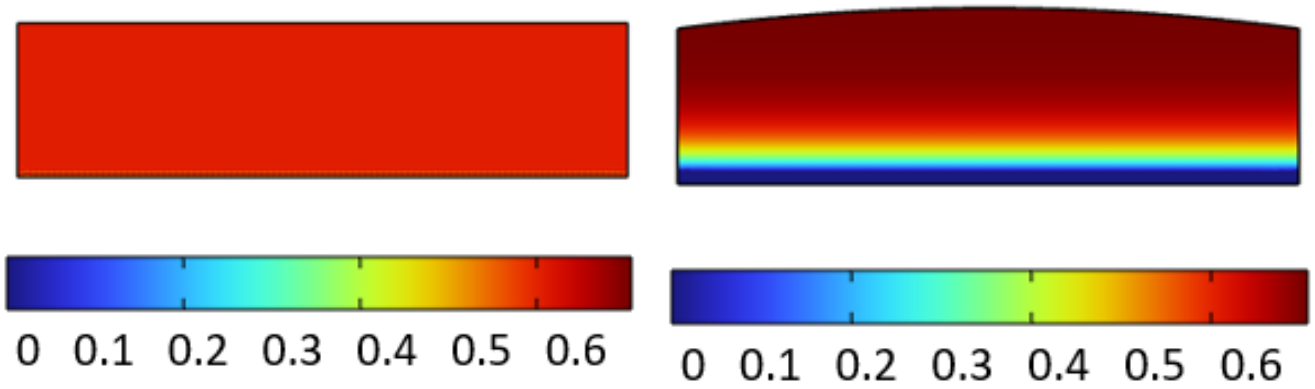

Figure 4.4: Moisture content at (t=0 mins) Moisture content at (t=15 mins)

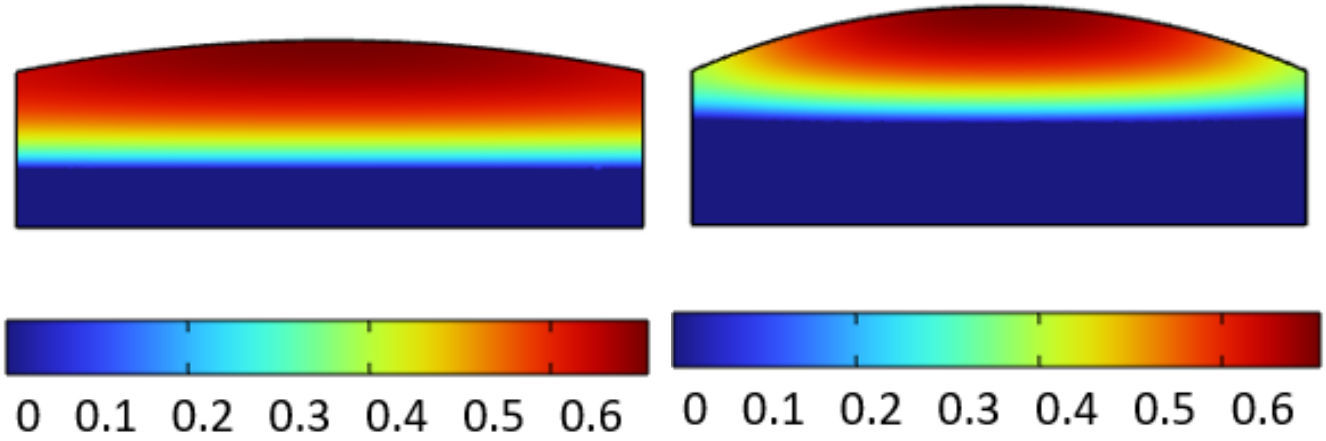

Figure 4.5: Moisture content at (t=30 mins) Moisture content at (t=45 mins)

At t = 0 mins, the red colour alone is spread throughout the structure of the dough. This is because the dough

is not yet subjected to any heat source. It means that the moisture content is the same throughout.

At t = 15 mins, there is a reduction in the moisture content which is seen at the bottom (blue colour) as a result of heat being applied during the baking process, more moisture content moves at the top (red colour). There is also evidence of cake expansion in height.

When t = 30 mins, it is evident that as baking time increases, the moisture content within the cake reduces. At this time, there is a more reduction in the moisture content level as compared to the previous times and a higher expansion of the cake in height.

After t = 45 mins, the moisture content is so low (reflected by a minimal red colour as compared to other colours). The blue colour dominates at this time implying there is more reduced moisture content level. These results are similar to what is reported by (Zhang & Datta, 2006; Cutté et al., 2016).

4.2.3 Illustration of how the level of moisture content changes with time

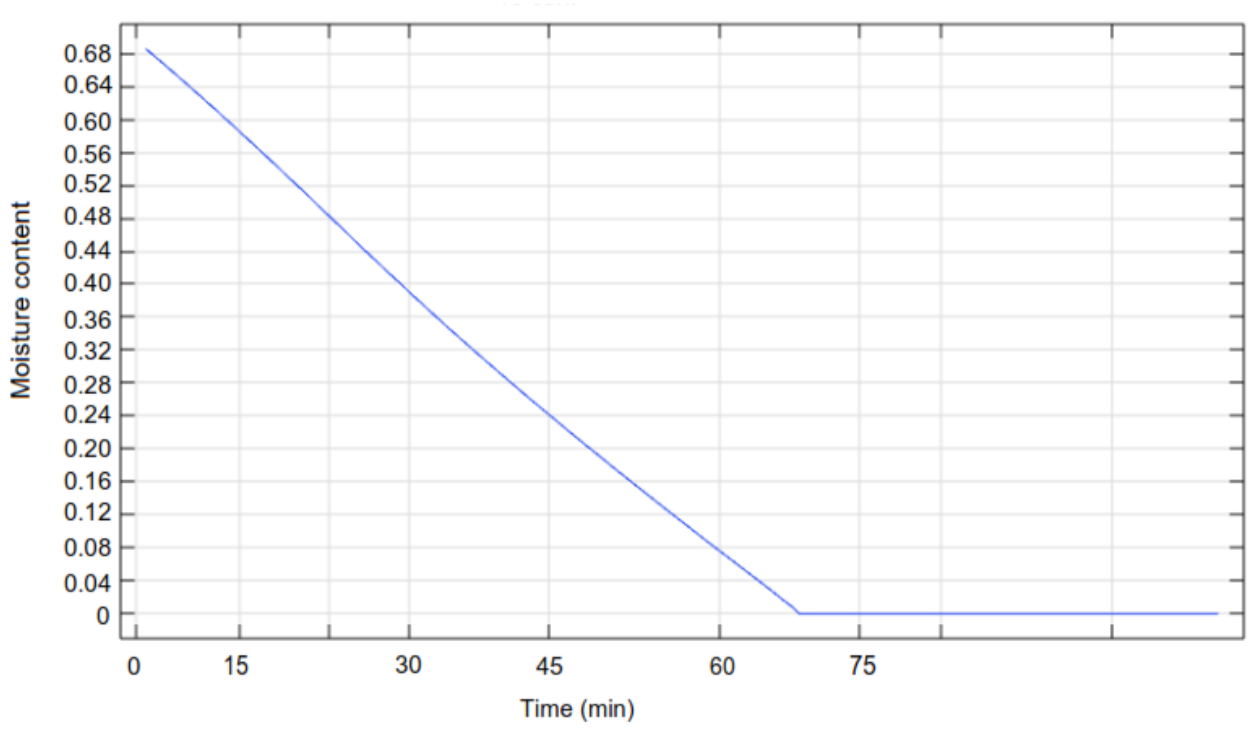

Figure 4.6: A graph of moisture content inside the cassava cake against time.

Figure 4.6 shows the variation of moisture with time. It reflects a decreasing trend with time. Initially, the moisture content level is close to 0.68 but as time goes on, it constantly reduces to 0 at 67.5 minutes. This is because of higher temperatures, which increase the kinetic energy of water molecules, enhancing the evaporation rate. The circulation of air also removes water vapour from the surface of the cake allowing more water to evaporate.

4.2.4 Illustration of cake expansion in height over time

The following graph in Figure 4.7 shows the expansion in height of a cassava cake over time during the baking process. The graph indicates a gradual rise and fall in the height of the cake at the start. This can be because of the

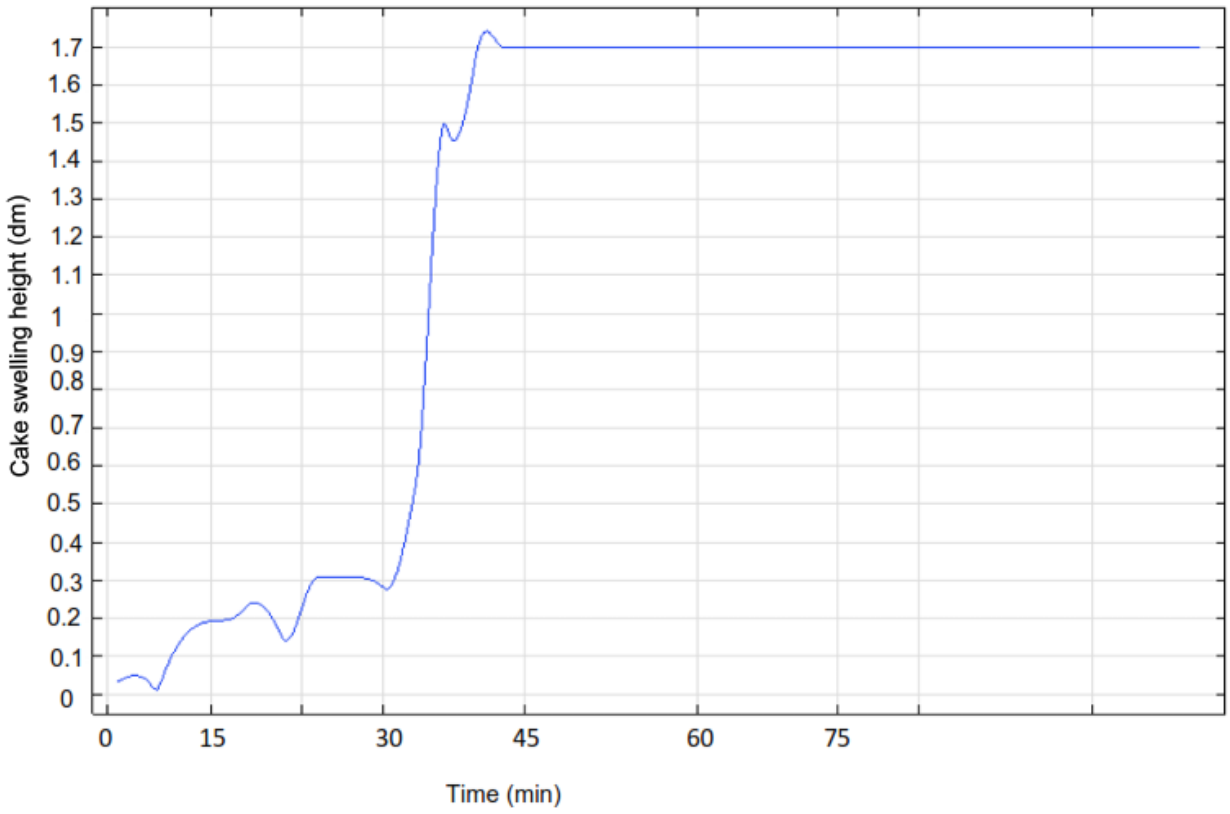

Figure 4.7: Height axes for the cake to see if there is expansion or not.

period when the yeast activation is still low (Zhang & Datta, 2006). This is followed by a steeper incline shortly after 30 minutes to 40 minutes, reaching a peak slightly above 1.7 dm. The graph then levels indicating stability of height of the cake swelling up to 75 minutes.

Initially, the increase in the height of the cake (expansion) is slow because at this stage, the dough has just been subjected to heat implying that the physio-chemical reactions responsible for the swelling are also taking place at a relatively lower rate.

The later on steeper incline shows a faster increase in the size of the cake which is caused by the higher rate at which the chemical and physical processes take place at this stage. This is due to a higher activation of the leavening agents like baking powder, the release of carbon dioxide which expands the cake batter, among others. When the cake reaches 1.75 dm, it then slightly drops back to a height of 1.7 dm and remains stable throughout.

A similar occurrence was portrayed in Cutté et al. (2016) which showed a maximum height of 26 mm at an approximate of 16 minutes after which the height of the cake remained constant. A large diffusivity also causes a faster loss in moisture content and hence resulting to an increased cake expansion (Zhang & Datta, 2006).

4.3 Results on Optimum Conditions

These refer to the cases under which the best cassava cake can be achieved during the baking process. In this study, the optimal baking time was 45 minutes at a temperature of 453 K. Also, cake expansion stops shortly after baking time of 45 minutes leaving a moisture content of 0.24 $KgKg^{-1}$.

Chapter 5

CONCLUSION AND RECOMMENDATIONS

5.1 CONCLUSION

A two dimensional model was formulated for the cassava cake baking process considering heat and mass transfer processes together with volume expansion (in terms of height). Simulation results were obtained regarding the temperature of the dough and moisture content profiles at a time interval of 15 minutes for 45 minutes. It was noticed that as the baking time increased, the moisture content within the dough kept reducing. There was also an observation that as baking time increased, the temperature distribution within the cassava cake dough also rose. Analysis about dough expansion in terms of height was made and it showed that shortly after the baking time of 45 minutes, the height of the cake remained constant.

This study successfully showed the potential of CFD in improving the baking process of cassava cake, pointing out its role in value addition. The key findings reveal that CFD simulations can effectively enhance critical baking parameters like temperature, time and moisture content leading to improved product quality. Additionally, this research emphasizes the importance of embracing innovative technologies like CFD in the food industry to improve food security and safety, support small scale farmers and food processors and also promote economic growth. Besides promoting the sustainable use of cassava flour, the study also contributes to its increased market value and also supports more efforts towards stability in the food sector.

Generally, the incorporation of CFD in food value addition offers a promising opportunity for enhancing both product quality and economic sustainability.

5.2 RECOMMENDATIONS

This research study provides key recommendations for improving cassava cake baking through the application of CFD and value addition techniques.

Since cassava flour is free from gluten, exploring new products like cassava cakes provides an option for people having celiac disease or those who are gluten sensitive, this study provides an alternative of cassava cakes as they meet different dietary needs especially for people avoiding gluten and also cater for diverse consumer preferences.

In addition, improving the mixing and blending of ingredients is also important for ensuring uniform moisture and temperature distribution.

For future studies, I recommend a case where temperature distribution within the oven, temperature distribution within the dough(cake) and moisture content and volume expansion can all be studied concurrently.

There is need for an experiment for the use of cassava flour in the baking process such that experimental results can be used to validate the model. these can also be used for comparison with simulation results.

References

Abass, A., Amaza, P., Bachwenkizi, B., Wanda, K., Agona, A., & Cromme, N. (2017). The impact of mechanized processing of cassava on farmers' production efficiency in uganda. *Applied Economics Letters*, *24*(2), 102–106.

Abdul Azeez, I. (2013). Cassava export and local utilization in nigeria top secrets. *The Consulting, Thursday May 30th*.

Adebayo, W. G. (2023). Cassava production in africa: A panel analysis of the drivers and trends. *Heliyon*, *9*(9).

Al-Nasser, M., Fayssal, I., & Moukalled, F. (2021). Numerical simulation of bread baking in a convection oven. *Applied Thermal Engineering*, *184*, 116–252.

Anandharamakrishnan, C., & Anandharamakrishnan, C. (2013). *Computational fluid dynamics applications in food processing*. Springer.

Ani, D., Ojila, H., & Abu, O. (2019). Profitability of cassava processing: A case study of otukpo lga, benue state, nigeria. *Sustain Food Prod*, *6*, 12–23.

Anishaparvin, A., Chhanwal, N., Indrani, D., Raghavarao, K., & Anandharamakrishnan, C. (2010). An investigation of bread-baking process in a pilot-scale electrical heating oven using computational fluid dynamics. *Journal of food science*, *75*(9), E605–E611.

Bárcenas, M. E., Altamirano-Fortoul, R., & Rosell, C. M. (2010). Effect of high pressure processing on wheat dough and bread characteristics. *LWT-Food Science and Technology*, *43*(1), 12–19.

Batchelor, G. K. (2000). *An introduction to fluid dynamics*. Cambridge university press.

Bayata, A. (2019). Review on nutritional value of cassava for use as a staple food. *Sci J Anal Chem*, *7*(4), 83–91.

Cevoli, C., Panarese, V., Catalogne, C., & Fabbri, A. (2020). Estimation of the effective moisture diffusivity in cake baking by the inversion of a finite element model. *Journal of Food Engineering*, *270*, 109–769.

Chakraborty, S., & Dash, K. K. (2023). A comprehensive review on heat and mass transfer simulation and measurement module during the baking process. *Applied Food Research*, *3*(1), 100–270.

Chakraborty, S., Routray, W., & Dash, K. K. (2022). Numerical study of baking. In *Advanced computational techniques for heat and mass transfer in food processing* (pp. 247–274). CRC Press.

Chhanwal, N., Indrani, D., Raghavarao, K., & Anandharamakrishnan, C. (2011). Computational fluid

dynamics modeling of bread baking process. *Food Research International*, *44*(4), 978–983.

Chhanwal, N., Moses, J., & Anandharamakrishnan, C. (2018). Improving bread-baking process under different oven load conditions by cfd modeling. In *Computational fluid dynamics in food processing* (pp. 225–242). CRC Press.

Chhanwal, N., Tank, A., Raghavarao, K., & Anandharamakrishnan, C. (2012). Computational fluid dynamics (cfd) modeling for bread baking process—a review. *Food and Bioprocess Technology*, *5*, 1157–1172.

Chisenga, S. M., Workneh, T. S., Bultosa, G., Alimi, B. A., & Siwela, M. (2020). Dough rheology and loaf quality of wheat-cassava bread using different cassava varieties and wheat substitution levels. *Food bioscience*, *34*, 100–529.

Cock, J. H., & Connor, D. J. (2021). Cassava. In *Crop physiology case histories for major crops* (pp. 588–633). Elsevier.

Cooke, R. D. (1978). An enzymatic assay for the total cyanide content of cassava (manihot esculenta crantz). *Journal of the Science of Food and Agriculture*, *29*(4), 345–352.

Cutté, R., Le Bideau, P., Glouannec, P., & Le Page, J. (2016). Numerical model for predicting heat and mass transfer phenomena during cake baking.

Davey, L., & Pham, Q. (1997). Predicting the dynamic product heat load and weight loss during beef chilling using a multi-region finite difference approach. *International Journal of Refrigeration*, *20*(7), 470–482.

Dziedzoave, N. (1998). Use of cassava flour in bakery products. final report for the first phase of the nri/fri cassava flour project. food research institute (fri), accra, ghana.

Fauquet, C., & Fargette, D. (1990). African cassava mosaic virus: etiology, epidemiology and control. *Plant Dis*, *74*(6), 404–411.

Haggblade, S., & Dewina, R. (2010). *Staple food prices in uganda* (Tech. Rep.).

Hu, Z., & Sun, D.-W. (2000). Cfd simulation of heat and moisture transfer for predicting cooling rate and weight loss of cooked ham during air-blast chilling process. *Journal of Food Engineering*, *46*(3), 189–197.

Jackson, J., & Chiwona-Karltun, L. (2018). Cassava production, processing and nutrition. *Handbook of vegetables and vegetable processing*, 609–632.

Kangarluei, A. R. (2015). Heat and mass transfer in industrial biscuit baking oven and effect of temper-

ature on baking time. *Journal of Heat and Mass Transfer Research*, *2*(2), 79–90.

Kapur, J. N. (2023). *Mathematical modeling*. Mercury Learning and Information. Retrieved from https://books.google.co.ug/books?id=C3iyEAAAQBAJ

Khan, S. A., Taj, F., Habib, S., Shawl, F., Dar, A. H., & Dwivedi, M. (2022). Cfd analysis of drying of cereal, fruits, and vegetables. In *Advanced computational techniques for heat and mass transfer in food processing* (pp. 235–246). CRC Press.

Khater, E.-S. G., & Bahnasawy, A. H. (2014). Heat and mass balance for baking process. *Journal of Bioprocessing & Biotechniques*, *4*(7), 1.

Khatir, Z., Paton, J., Thompson, H., Kapur, N., Toropov, V., Lawes, M., & Kirk, D. (2023). Computational fluid dynamics (cfd) investigation of air flow and temperature distribution in a small scale bread-baking oven. *Applied Energy*, *89*(1), 89–96.

Kianmehr, H. (1995). Research scientist and assistant professor, agriculture and agri-food canada, 430 gouin boul, st-jean-sur-richelieu, quebec, canada, i 3b 3e6, and depart-ment of plant science, mcgill university, 21 111 lakeshore road, ste-anne. *Journal of Plant Nutrition*, *18*(6), 1073–1079.

Kuye, O., & Ettah, O. (2016). Contributions of urban mixed-cropping to household food security in nigeria and around the globe. *International Journal of Environment, Agriculture and Biotechnology*, *1*(2), 238–531.

Li, M., Zhang, Y., You, X., Wang, Y., Zhou, K., Wei, P., & Wei, L. (2023). Assessment of functional properties of wheat–cassava composite flour. *Foods*, *12*(19), 35–85.

Lintermann, A. (2021). Computational meshing for cfd simulations. *Clinical and biomedical engineering in the human nose: A computational fluid dynamics approach*, 85–115.

Maduagwu, E., & Adewale, A. (1981). Loss of hydrocyanic acid and its derivatives during sun drying of cassava. In *Tropical root crops: research strategies for the 1980s: proceedings of the first triennial root crops symposium of the international society for tropical root crops-africa branch, 8-12 sept. 1980, ibadan, nigeria.*

Mahungu, N., Yamaguchi, Y., Almazan, A., & Hahn, S. (1987). Reduction of cyanide during processing of cassava into some traditional african foods. *J. Food Agric*, *1*(1), 11–15.

Mirade, P.-S., Daudin, J.-D., Ducept, F., Trystram, G., & Clément, J. (2004). Characterization and cfd modelling of air temperature and velocity profiles in an industrial biscuit baking tunnel oven. *Food research international*, *37*(10), 1031–1039.

Moureh, J., & Derens, E. (2000). Numerical modelling of the temperature increase in frozen food packaged in pallets in the distribution chain. *International Journal of Refrigeration*, *23*(7), 540–552.

Mwape, M. C., Parmar, A., Roman, F., Azouma, Y. O., Emmambux, N. M., & Hensel, O. (2023). Determination and modeling of proximate and thermal properties of de-watered cassava mash (manihot esculenta crantz) and gari (gelatinized cassava mash) traditionally processed (in situ) in togo. *Energies*, *16*(19), 1–22.

Navacchi, M. F. P., de Carvalho, J. C. M., Takeuchi, K. P., & Danesi, E. D. G. (2012). Development of cassava cake enriched with its own bran and spirulina platensis. *Acta Scientiarum. Technology*, *34*(4), 465–472.

Nicolas, V., Salagnac, P., Glouannec, P., Jury, V., Boillereaux, L., & Ploteau, J. P. (2010). Modeling heat and mass transfer in bread during baking. In *Comsol conference.*

Norton, T., & Sun, D.-W. (2006). Computational fluid dynamics (cfd)–an effective and efficient design and analysis tool for the food industry: a review. *Trends in Food Science & Technology*, *17*(11), 600–620.

Odebode, S. O. (2008). Appropriate technology for cassava processing in nigeria: User's point of view. *Journal of International Women's Studies*, *9*(3), 269–286.

Oladunmoye, O. O., Aworh, O. C., Maziya-Dixon, B., Erukainure, O. L., & Elemo, G. N. (2014). Chemical and functional properties of cassava starch, durum wheat semolina flour, and their blends. *Food science & nutrition*, *2*(2), 132–138.

Onwueme, I. (1978). Evaluation of the performance of cassava (manihot esculenta crantz) when grown from inverted stem cuttings. *The Journal of Agricultural Science*, *90*(1), 149–156.

Orias, R. R., & Calub Jr, F. C. (1986). Evaluation of primary ppocessin; techniques on local cassava pi ou production using the pedal. op rated. *Ann. Trop. Res*, *8*, 61–71.

Panghal, A., Munezero, C., Sharma, P., & Chhikara, N. (2019). Cassava toxicity, detoxification and its food applications: a review. *Toxin Reviews*.

Park, H. W., & Yoon, W. B. (2018). Computational fluid dynamics (cfd) modelling and application for sterilization of foods: A review. *Processes*, *6*(6), 62.

Parmar, A., Sturm, B., & Hensel, O. (2017). Crops that feed the world: Production and improvement of cassava for food, feed, and industrial uses. *Food Security*, *9*, 907–927.

Rahman, S. A., Nassef, A. M., Rezk, H., Assad, M. E. H., & Hoque, M. E. (2021). Experimental investigations and modeling of vacuum oven process using several semi-empirical models and a fuzzy model of cocoa beans. *Heat and Mass Transfer*, *57*, 175–188.

Rogers, D. J. (1963). Studies of manihot esculenta crantz and related species. *Bulletin of the Torrey Botanical Club*, 43–54.

Sadeghi, F., Hamdami, N., Shahedi, M., & Rafe, A. (2016). Numerical modeling of heat and mass transfer during contact baking of flat bread. *Journal of Food Process Engineering*, *39*(4), 345–356.

Scott, G., & Richardson, P. (1997). The application of computational fluid dynamics in the food industry. *Trends in Food Science & Technology*, *8*(4), 119–124.

Sengar, R. (2022). Cassava processing and its food application: A review.

Sharma, A. (2021). *Introduction to computational fluid dynamics: development, application and analysis*. Springer Nature.

Shittu, T. A., Alimi, B. A., Wahab, B., Sanni, L. O., & Abass, A. B. (2016). Cassava flour and starch: Processing technology and utilization. *Tropical roots and tubers: Production, processing and technology*, 415–450.

Süfer, Ö., Kumcuoğlu, S., & Tavman, . (2016). Modeling heat and mass transfer in cakes and other bakery products during baking and computational fluid dynamics (cfd) applications. *Akademik Gida*, *14*(1), 61–66.

Szpicer, A., Bińkowska, W., Wojtasik-Kalinowska, I., Salih, S. M., & Półtorak, A. (2023). Application of computational fluid dynamics simulations in food industry. *European Food Research and Technology*, *249*(6), 1411–1430.

Tank, A., Chhanwal, N., Indrani, D., & Anandharamakrishnan, C. (2014). Computational fluid dynamics modeling of bun baking process under different oven load conditions. *Journal of food science and technology*, *51*, 2030–2037.

Therdthai, N., Zhou, W., & Adamczak, T. (2002). Optimisation of the temperature profile in bread baking. *Journal of Food Engineering*, *55*(1), 41–48.

Therdthai, N., Zhou, W., & Adamczak, T. (2004). Three-dimensional cfd modelling and simulation of the temperature profiles and airflow patterns during a continuous industrial baking process. *Journal of Food Engineering*, *65*(4), 599–608.

Tien, N. N. T., Duyen, T. T. M., & Hung, P. V. (2019). Substitution of wheat flour with highly enzyme-resisted cassava starch and its effect on starch digestibility and quality of breads. *Journal of Food Measurement and Characterization*, *13*(2), 1004–1010.

Trystram, G. (2012). Modelling of food and food processes. *Journal of Food Engineering*, *110*(2), 269–277.

Tu, J., Yeoh, G. H., Liu, C., & Tao, Y. (2023). *Computational fluid dynamics: a practical approach*. Elsevier.

Ubalua, A. O., & Mbanaso, E. (2013). A novelgene transformation technique for farmer's preferred cassava cultivar (nwibibi) from nigeria. *World Journal of Agricultural Sciences*, *9*(3), 284–289.

Uchechukwu-Agua, A. D., Caleb, O. J., & Opara, U. L. (2015). Postharvest handling and storage of fresh cassava root and products: a review. *Food and Bioprocess Technology*, *8*, 729–748.

Unteawati, B., & Fatih, C. (2018). Consumer's market analysis of products based on cassava. In *Iop conference series: Earth and environmental science* (Vol. 141, pp. 12–33).

Velten, K., Schmidt, D. M., & Kahlen, K. (2024). *Mathematical modeling and simulation: introduction for scientists and engineers*. John Wiley & Sons.

Versteeg, H., & Malalasekera, W. (1995). Computational fluid dynamics. *The finite volume method*, 1–26.

White, F. M., & Majdalani, J. (2006). *Viscous fluid flow* (Vol. 3). McGraw-Hill New York.

Wong, S. Y., Zhou, W., & Hua, J. (2006). Robustness analysis of a cfd model to the uncertainties in its physical properties for a bread baking process. *Journal of Food Engineering*, *77*(4), 784–791.

Xia, B., & Sun, D.-W. (2002). Applications of computational fluid dynamics (cfd) in the food industry: a review. *Computers and electronics in agriculture*, *34*(1-3), 5–24.

Yan, Y., & Tu, J. (2023). Computational fluid dynamics. In *Bioaerosol characterisation, transportation and transmission: Fundamental, modelling and application* (pp. 65–83). Springer.

Yanniotis, S., & Stoforos, N. (2014). Modeling food processing operations with computational fluid dynamics: A review. *Scientia agriculturae bohemica*, *45*(1), 1–10.

Zanoni, B., Peri, C., & Bruno, D. (1995). Modelling of starch gelatinization kinetics of bread crumb during baking. *LWT-Food Science and Technology*, *28*(3), 314–318.

Zhang, J., & Datta, A. (2006). Mathematical modeling of bread baking process. *Journal of Food Engineering*, *75*(1), 78–89.

Zhou, W., & Therdthai, N. (2018). Three-dimensional cfd modeling of continuous industrial baking process. In *Computational fluid dynamics in food processing* (pp. 193–224). CRC Press.